CAPITAL UNIVERSITY OF SCIENCE AND TECHNOLOGY, ISLAMABAD

Green Synthesis and *In-vivo* Toxicity Assessment of Magnesium Sulfide Nanoparticles in Sprague Dawley Rat Model

by

Muhammad Hamza Masood

A thesis submitted in partial fulfillment for the degree of Master of Science

in the

Faculty of Health and Life Sciences
Department of Bioinformatics and Biosciences

2025

My path has been built on the strength, sacrifices, and unending support of parents, to whom I dedicate my thesis. My academic career was shaped by my instructors and mentors, for whom I am incredibly thankful. I want to express my gratitude to my friends for their encouragement. And to my devoted wife, whose understanding, patience, and unwavering support enabled me to keep going, this accomplishment is equally yours as it is mine.

CERTIFICATE OF APPROVAL

Green Synthesis and *In-vivo* Toxicity Assessment of Magnesium Sulfide Nanoparticles in Sprague Dawley Rat Model

by

Muhammad Hamza Masood

(MBS233018)

THESIS EXAMINING COMMITTEE

S. No.	Examiner	Name	Organization
(a)	External Examiner	Dr. Masood Ur Rehman Kayani	NUST, Islamabad
(b)	Internal Examiner	Dr. M. Asad Anwar	CUST, Islamabad
(c)	Supervisor	Dr. Sania Riaz	CUST, Islamabad

Dr. Sania Riaz
Thesis Supervisor
September, 2025

Dr. Syeda Marriam Bakhtiar
Head
Dept. of Bioinfo. & Biosciences
September, 2025

Dr. Sahar Fazal
Dean
Faculty of Health & Life Sciences
September, 2025

Author's Declaration

I, **Muhammad Hamza Masood** hereby state that my MS thesis titled "**Green Synthesis and *In-vivo* Toxicity Assessment of Magnesium Sulfide Nanoparticles in Sprague Dawley Rat Model**" is my own work and has not been submitted previously by me for taking any degree from Capital University of Science and Technology, Islamabad or anywhere else in the country/abroad.

At any time if my statement is found to be incorrect even after my graduation, the University has the right to withdraw my MS Degree.

(Muhammad Hamza Masood)
Registration No: MBS233018

Plagiarism Undertaking

I solemnly declare that research work presented in this thesis titled "**Green Synthesis and *In-vivo* Toxicity Assessment of Magnesium Sulfide Nanoparticles in Sprague Dawley Rat Model**" is solely my research work with no significant contribution from any other person. Small contribution/help wherever taken has been duly acknowledged and that complete thesis has been written by me.

I understand the zero tolerance policy of the HEC and Capital University of Science and Technology towards plagiarism. Therefore, I as an author of the above titled thesis declare that no portion of my thesis has been plagiarized and any material used as reference is properly referred/cited.

I undertake that if I am found guilty of any formal plagiarism in the above titled thesis even after award of MS Degree, the University reserves the right to withdraw/revoke my MS degree and that HEC and the University have the right to publish my name on the HEC/University website on which names of students are placed who submitted plagiarized work.

Hamza

(Muhammad Hamza Masood)
Registration No: MBS233018

Acknowledgement

Above all, I want to express my sincere gratitude to Allah Almighty for giving me the courage, endurance, and direction I needed to finish my thesis. My sincere gratitude goes out to my supervisor, Dr. Sania Riaz, for her helpful advice, unwavering support, and knowledgeable insight along my research journey. This work was greatly influenced by her support and helpful criticism.

I want to express my gratitude to my family, whose love, prayers, and unwavering support have given me strength. Even at the most trying circumstances, their unshakeable faith in me inspired me to keep going forward. I acknowledge the Department of Bioinformatics and Biosciences for providing me with the necessary resources and support to pursue my research.

I am also grateful to my friends, who supported me throughout my academic journey by offering timely humor, understanding, and encouragement.

Thanks to all.

(Muhammad Hamza Masood)

Abstract

Nanoparticles possess unique physicochemical properties that can lead to significant biological interactions, including potential toxicity. In this study, magnesium sulfide nanoparticles (MgS-NPs) were synthesized via a green route using *Citrus limetta* leaf extract, which served as a natural reducing and stabilizing agent due to its rich phytochemical content. They were confirmed by SEM and XRD analyses to be crystalline in morphology, and within the nanoscale range of 80- 120nm. The synthesized nanoparticles were characterized using UV-Visible spectroscopy, FTIR, SEM, EDX, and XRD to confirm their optical properties, functional groups, morphology, elemental composition, and crystalline structure. To assess in-vivo toxicity, MgS-NPs were orally administered to Sprague-Dawley rats at two dose levels low (1.73 mg/200g) and high (3.46 mg/200g) over a 20-day period. The evaluation included hematological, biochemical, and histopathological analyses to determine dose-dependent effects. Hematological analysis revealed that high-dose administration significantly decreased red blood cells, hemoglobin, and platelet counts while elevating white blood cell levels, indicating anemia, coagulopathy, and systemic inflammatory response. Significant alterations were observed in several hematological and biochemical markers in the treated groups compared to the control group ($p < 0.05$, one-way ANOVA). The high-dose group exhibited elevated ALT, AST, urea, and creatinine levels, along with decreased RBC and platelet counts, indicating hepatic and renal stress. Histopathological examination revealed in high-dose group it exhibits hepatocellular degeneration, vacuolization, nuclear pyknosis, and moderate inflammatory infiltration in liver tissues, while kidneys displayed glomerular shrinkage, tubular necrosis, and disrupted architecture. In contrast, the low-dose group exhibited only mild vacuolar degeneration and limited tissue alterations, suggesting comparatively lower toxicity and better biocompatibility. These findings highlight the importance of dose consideration in the biomedical application of green-synthesized MgS nanoparticles. Although the green synthesis approach enhances biocompatibility, prolonged or high-dose exposure may still pose risks to vital organs. Therefore, further studies focusing on long-term exposure, biodistribution, and molecular mechanisms are essential

to establish a comprehensive safety profile for MgS-NPs in clinical or therapeutic use.

Keywords: Magnesium Sulfide Nanoparticles, Green Synthesis, Citrus Limetta, In-Vivo Toxicity, Dose-Dependent Response, Hepatotoxicity, Nephrotoxicity, Oxidative Stress, Biochemical Markers, Histopathology, Phytochemical Stabilization, Nanomedicine Safety.

Contents

List of Figures

List of Tables

Abbreviations

ALP	Alkaline phosphataseb
ALT	Alanine transaminase
AST	Aspartate aminotransferase
CT SCAN	Computed Tomography Scan
EDTA	Ethylenediaminetetraacetic acid
EDX	Energy dispersive X-ray
EOS	Eosinophils
FTIR	Fourier-transform infrared spectroscopy
Hb	Hemoglobin
IST	Institute of space and technology
LFT	Liver function test
LYMPHO	Lymphocytes
MCH	Mean corpuscular hemoglobin
MCHC	Mean corpuscular hemoglobin concentration
MCV	Mean corpuscular volume
MONO	Monocytes
MRI	Magnetic Resonance Imaging
MgS-NPs	Magnesium Sulfide nanoparticles
NBF	Neutral-buffered formaldehyde
NEU	Neutrophils
PET SCAN	Positron Emission Tomography
PLT	Platelets
RBC	Red blood cells
RFT	Renal function test

ROS	Reactive oxygen Species
SEM	Scanning electron microscopy
UV-Vis spectroscopy	Ultraviolet -Visible Spectroscopy
WBC	White blood cells
XRD	X-ray diffraction

Chapter 1

Introduction

Nanoparticles are particles with sizes ranging from 1nm to 100nm. They can also be categorized based on their composition, special qualities, or shape. These days, nanotechnology is widely used in many sectors, particularly by environmental and health specialists. Their production and effects on biological systems have generated a great deal of curiosity and contribution, making this topic one of the most fascinating research fields that has garnered attention [1]. Better catalytic, magnetic, electrical, mechanical, optical, chemical, and biological qualities are displayed by particles in the nanoscale. NPs have greater reactivity, mobility, dissolving characteristics, and strength because of their high surface to volume ratio [2].

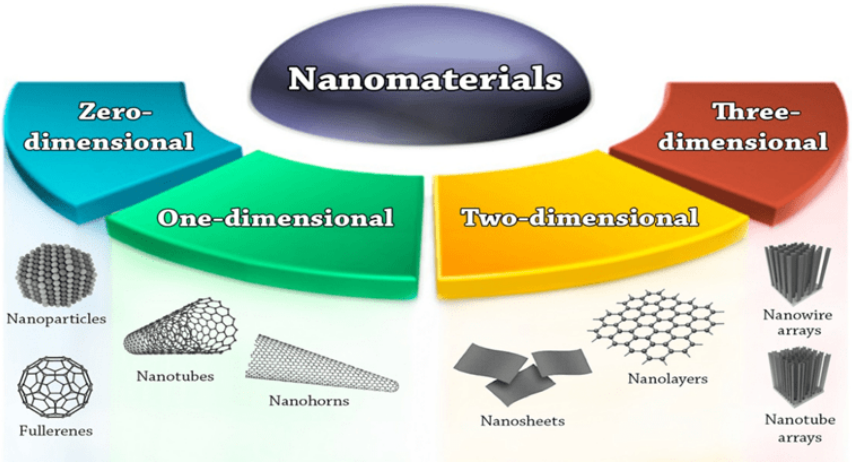

FIGURE 1.1: Nanomaterials classification based on dimensionality [3]

Even though particles' crystalline forms often lead to multifarious shapes, they are usually examined and described as spheres or rods. Environmental science, electronics, medicine, and energy are only a few of the sectors it could revolutionize, providing solutions to critical problems and opening new avenues for technological advancement and scientific research. Surface chemistry of nanoparticles cam be adjusted to attain particular function by improving their efficacy in biocatalysis, drug administration and environmental sensing [4]. There are wide range applications of different nanoparticles in biology, engineering and medicine. For example, Gold NPs have antimicrobial properties and have applications in enzyme regulation. Silver NPs inhibit growth of gram positive and negative bacteria. Iron NPs show antimicrobial properties and used for the cleaning of contamination [5]. According to reports in past few years many types of metal nanoparticles are synthesized for various applications due to their biocompatibility, ultra small size localized plasmon resonance etc. Zirconium nanoparticles are designed to detect vitamin C in environmental and food samples [6]. Cerium oxide nanoparticles, commonly known as nanoceria have unique morphology which makes them excellent material in biological fields such as neuroprotection, radiotherapy and antioxidant therapy [7].

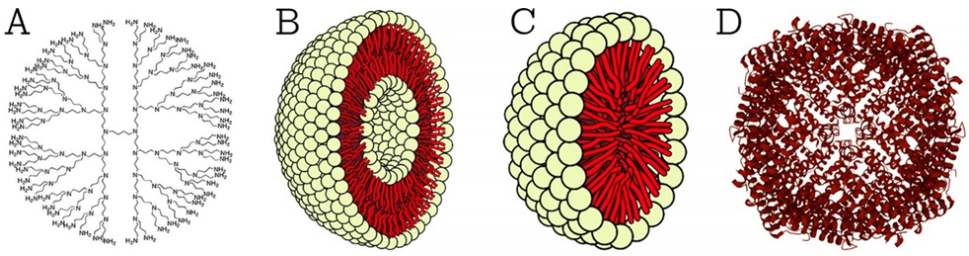

FIGURE 1.2: The image illustrates various nanostructures commonly used in drug delivery and nanomedicine. Panel A shows a dendrimer Panels B and C depict liposome and micelle-like structures. Finally, D represents a protein-based nanoparticle, composed of complex folded protein subunits forming a symmetric nanocage [3]

Green synthesis techniques are being emphasized in advanced material sciences research as a means of purifying and restoring nanomaterials to increase their ecological sustainability [8]. Green synthesized metallic nanoparticles can be synthesized from bacteria, fungi and algae but for larger quantities using plant extract

is much easier and convenient as compared to microbes. To attain this appropriate solvent systems and natural resources are needed [9]. Nanoparticles can cause toxicity because of their high reactivity due to higher surface area which can interfere with normal biological functions. Reactive oxygen species generated by NPs results in oxidative stress that disrupts lipids, proteins and DNA in a cell [10].

Understanding nanotoxicity is essential to grasping long-term effects, especially for consumers purchasing products containing nanoparticles and workers in organizations using nanomaterial. To ensure safety, compliance, and the responsible development of nanotechnology, it is crucial to comprehend nanotoxicity. It is essential for safeguarding both the environment and human health while facilitating the development of novel materials and application [10].

Magnesium Oxide nanoparticles are applied in tumor inhibition and also are antimicrobial agents. The percentage of free radical scavenging in synthesized MgO NPs derived from Abrus precatorius bark was greater. The toxicity of the produced MgO nanoparticles was evaluated using zebrafish embryos as a model organism; the findings indicated that the MgO NPs were harmless. Additionally, a human melanoma cancer cell line (A375) was used to assess the anticancer effects of MgO nanoparticles [11].

A visible zone of inhibition is observed against E. coli, P. aeruginosa and S. aureus MgO Nps synthesized by neem leaves extract [12]. MgO nanoparticles in vivo toxicity studies in rats showed increased level of aspartate aminotransferase and alkaline phosphatase, also increases RBCs, WBCs and Hemoglobin as compared to control. It was found out that concentration below 250 μg.mL-1 are safer to use for desired applications [13]. Cytotoxic studies of Magnesium hydroxide nanoparticles on rats revealed that repeated exposure to these NPs have adverse effects on kidney and liver. Exposure to these NPs results in increased AST, ALP and creatinine levels and reduction in albumin, globulin and hepatic total proteins [14].

Biologically synthesized Cadmium sulfide nanoparticles showed antimicrobial activity against pathogens like *Aspergillus fumigatus, Aspergillus niger, Geotricum*

candidum, and *Candida albicans, Bacillus subtilis, Streptococcus pneumoniae, Staphylococcus aureus* and *Staphylococcus epidermidi* [15]. Rats treated with Cd-SNPs also had higher creatinine concentrations in their urine. Proximal tubules showed significant damage, according to histopathological studies.

Ultrastructural analyses revealed alterations in the endoplasmic reticulum, nuclear, and mitochondria. Their unique physicochemical characteristics, increased capacity to produce ROS, development of oxidative stress, and impairment of renal structure and function have all been linked to these effect [16]. Lead sulfide nanoparticles can cause oxidative damage and inflammatory response in lungs and also it causes damage to rat kidney tissues [16].

Eco friendly green synthesized Magnesium nanoparticles are also reported to be prepared by extract of barley seeds. Green synthesized MgS-NPs from *Punica granatum* seeds extract showed effective activity against neuroblastoma cell line and prevented their proliferation [17]. Magnesium sulfide nanoparticles are safer to be utilized as compared to others because Mg ions are used as co-factors by kinases and phosphorylases and Sulphur is the part of different amino acids that are the building blocks of proteins [18].

Because they exist in the nano-form and induce oxidative stress in many cells, nanoparticles can interact with a wide range of biological materials in various ways and accumulate to produce their harmful effect. Unfortunately, little is known about how long-term exposure to nanoparticles affects both the environment and human health. The effects of nanoparticles on the environment and human health should be further evaluated before they are produced on a wide scale and used in a variety of industries [19].

1.1 Problem Statement

Serious homeostasis disruptions brought on by prolonged systemic exposure to green synthesized MgS-NPs may have an adverse effect on hematological markers and overall health. In many organs, elevated oxidative stress and inflammation can

impair organ function and increase long-term health concerns. The safety profile of these nanoparticles needs to be further investigated, especially in relation to their long-term exposure and biocompatibility in biological systems.

1.2 Hypothesis

Green synthesized MgS nanoparticles using Citrus limetta leaves extract may have immunological, biochemical or histopathological toxicity.

1.3 Gap Analysis

There are few studies regarding the green synthesis of MgS-NPs and their effectiveness against neuroblastoma cell line but there is lack of information regarding toxicity of MgS-NPs and their effect on biological systems. There are no studies present to address antimicrobial properties of green synthesized MgS-NPs. Also, no information is available concerning green synthesis of MgS-NPs from Citrus limetta and their interaction with biological systems. So, this is the significant gap and filling this gap is essential for the safe use of *Citrus limetta* synthesized MgS-NPs for biomedical applications.

1.4 Aim and Objectives

The aim of the study is to synthesized Mg NPs using Citrus limetta leaves extract and to check their safety profile. It will be aligned by following objectives:

- To synthesize and characterize the MgS-NPs from *Citrus limetta* leaves extract
- To check the effects of Green-synthesized MgS-NPs on Rat Model
- To evaluate the in-vivo toxicity and safety profile of Green-synthesized MgS-NPs using biochemical, histopathological and hematological response of rats after intake of Green-synthesized MgS-NPs nanoparticles.

Chapter 2

Literature Review

2.1 Nanotechnology and Nanomedicine

Nanotechnology is capable of helping create materials with better properties, such as increased strength, decreased weight, and enhanced chemical resistance. In nanomedicine, an aspect of nanotechnology in healthcare, nanoparticles, which have sizes ranging from 1 to 100 nm, interact with biological molecules on the surface and inside of cells. Drugs and medications can be administered directly to certain cells, including cancer cells, with the use of nanoparticles, which lowers adverse effects and increases effectiveness [20].

NPs improve drug stability, bioavailability, targeted distribution, and the duration of the drug's action in the target tissue, among other aspects of drug efficiency and safety. These particles are further separated into two categories: nanodrugs and nanocarriers. Nanoparticles can reach a wider variety of cellular and intracellular targets than microparticles because of their smaller size and greater mobility [21].

2.2 Properties of Nanoparticles

A variety of distinct physicochemical characteristics set nanoparticles apart from bulk materials. Their tiny size, usually ranging from 1 to 100 nanometers, is one of

their most distinctive characteristics. This leads to a high surface area-to-volume ratio, which improves their biological interactions and chemical reactivity. Their morphology—whether spherical, rod-shaped, or cubic—influences their interactions with other materials and cells. Zeta potential, a measure of surface charge, is essential for colloidal stability; nanoparticles with values higher than ±30 mV are regarded as stable in suspension. Using methods like X-ray diffraction (XRD), their crystalline structure and phase may be determined, providing crucial details regarding their mechanical and optical characteristics. Energy Dispersive X-ray Spectroscopy (EDX), which measures chemical composition, verifies the existence of core components and any surface alterations. Furthermore, nanoparticles frequently have special optical characteristics that may be examined with UV-Vis spectroscopy, such as surface plasmon resonance in metallic nanoparticles. Additionally, their surfaces could have FTIR-detectable functional groups (such as -OH, -COOH, and -NH_2) that are essential for stabilization, targeting, or drug administration. Additionally, their suitability for use in industrial and biological contexts is influenced by their dispersibility, solubility, and aggregation behaviour in different solvents. These traits together determine the efficacy, safety, and functioning of nanoparticles in a range of technical and scientific applications [22].

2.2.1 Size of Nanoparticles

Since it affects biological destiny, toxicity, in vivo distribution, and targeting ability, particle size is one of the most crucial characteristics of NPs. Additionally, the NPs have an impact on drug loading, stability, and release. Drug release depends on particle size. Drug release is accelerated by small particles' greater surface area-to-volume ratio. On the other hand, because of their huge cores, larger particles enable the extra drug to be encapsulated per particle, leading to a slower rate of drug release [21].

2.2.2 Particle Shape

The incorporation of nanoparticles by the targeted cells makes their physical shape vital to biodistribution. Cationic nanoparticles with a rod shape, for example,

are simpler for endosomes to absorb than those with other shapes, indicating that immune system cells may perceive them as rod-shaped germs. Therapeutic nanoparticles' surface charge is crucial to their precise distribution and clearance. The immune system reacts more strongly to positively charged nanoparticles than to neutral or negatively charged ones [23].

2.2.3 Surface Hydrophobicity

It is also believed that hydrophobicity is a crucial factor in predicting how nanomaterials would behave in the environment and interact with biological systems. Similar to chemicals, hydrophilic nanoparticles have a higher chance of staying in the water column and maybe having greater mobility, while hydrophobic particles are more likely to adhere to organic matter in the sediment. NPs are frequently functionalized with different surface coatings, which can change how hydrophobic the surface is.

According to earlier research, modifications in the particle surface's hydrophobicity can influence cell contacts and, in turn, absorption. According to a different study, the hydrophobicity of coatings (citrate, PVP, and GA) was directly correlated with the attachment of Ag NPs to hydrophobic collector surfaces. As a result, a practical hydrophobicity metric that appropriately captures the intricate and dynamic behaviour of NPs is required [24].

2.2.4 Drug Release

The solubility of the drugs, the rate at which the adsorbed drug dissolves, the drug's diffusion via nanoparticle matrices, the degradation or erosion of the nanoparticle matrixes, and the combination of the diffusion and erosion processes are the main factors that affect the release rate of the drugs.

sRelease is significantly governed by the diffusion process if it outpaces matrix erosion in speed. The drug is consistently dispersed and delivered in nanospheres through diffusion or matrix erosion [25].

2.2.5 Targeted Delivery of Nanoparticles

NPs must be able to reach the expected site of action or tumor site with the least amount of activity or volume loss in order for an anti-cancer medication delivery system to be effective. Second, they must be able to produce the intended therapeutic effect after they have entered the tumor site. In both cases, nanoparticles meet these criteria. NPs must always arrive at the target location correctly. Once there, they must bind to the site, transfer the drug materials to the targeted tissues, and lessen the harm that the medications do to healthy cells. Keeping the coating-specific ligands on the NPs' surface is the most popular tactic. Small compounds, proteins, antibodies, and nucleic acid aptamers can all create this ligand [26].

2.3 Synthesis of Nanoparticles

There are two main approaches for the synthesis of Nanoparticles.

2.3.1 Top-Down Approach

To create the necessary nanostructure, the "top-down" method breaks down the big material fragments. Top-down methods can produce particles with defects and less control over their size and shape, despite being scalable and very simple to employ. Ball milling crushes particles at the nanoscale using a top-down method, whereas lithography uses to create the necessary nanostructure, the "top-down" method breaks down the big material fragments. Top-down methods can produce particles with defects and less control over their size and shape, despite being scalable and very simple to employ.

2.3.2 Bottom-up Approach

Usually through chemical or biological synthesis, the bottom-up strategy involves molecules self-assembling and building up to form nanostructures or nanoparticles atom by atom or molecule by molecule. Bottom-up methods usually provide better control over the size, composition, and structure of nanoparticles and are often

more economically and ecologically efficient, but they can be challenging to scale up consistently.

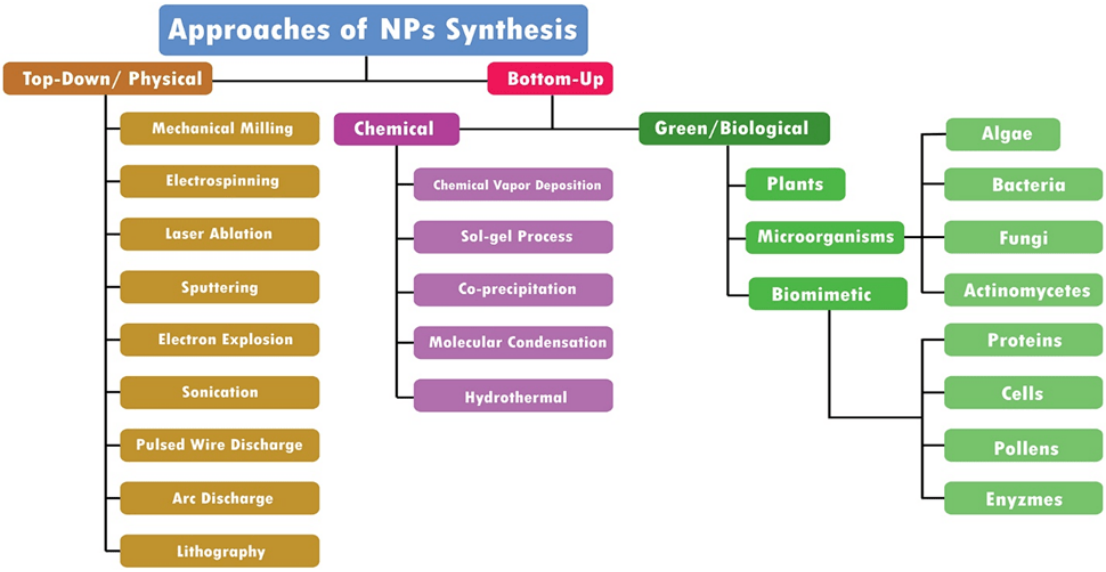

FIGURE 2.1: Approaches to synthesize Nanoparticles [27]

2.4 Types of Nanoparticles

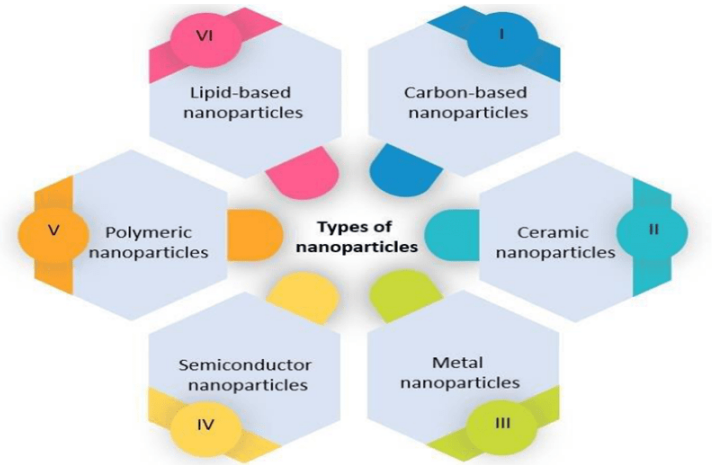

FIGURE 2.2: Different types of Nanoparticles

2.4.1 Carbon Based Nanoparticles

Fullerenes and carbon nanotubes (CNTs) are the two main subgroups of carbon-based NPs. NPs of spherical hollow cages, which mimic allotropic forms of carbon,

are found in fullerenes. Their exceptional strength, structure, electron affinity, electrical conductivity, and flexibility have garnered significant commercial interest [28].

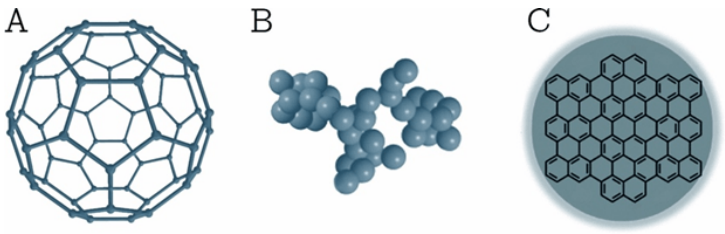

FIGURE 2.3: Different types of carbon-based nanoparticles: C60 fullerene, carbon black, and carbon quantum dots, each with distinct structures and properties [29]

Carbon-based nanoparticles come in a variety of structural forms, each offering distinct physicochemical properties suited to different applications. Spherical fullerenes feature a highly organized, cage-like arrangement of carbon atoms that provides remarkable stability and electron-accepting capabilities. In contrast, carbon dots are composed of loosely packed clusters of carbon atoms with more irregular shapes, known for their small size, high surface area, and intrinsic fluorescence, making them ideal for imaging and biosensing. Graphene quantum dots, on the other hand, are flat, nanoscale fragments of graphene sheets with a defined hexagonal carbon lattice. Their unique combination of conductivity, biocompatibility, and edge chemistry makes them especially useful in drug delivery systems, bioimaging, and energy-related technologies.

2.4.2 Metallic Nanoparticles

Metal nanoparticles are composed entirely of metals. These NPs' well-known localized surface Plasmon resonance (LSPR) characteristics give them unique electrical characteristics. A wide absorption band is seen in the visible portion of the solar electromagnetic spectrum in Cu, Ag, and Au nanoparticles. Because of their improved characteristics, such as their regulated production in terms of size, shape, and facet, metal nanoparticles are employed in a variety of scientific domains.

Due to their optical, electrical, and molecular-recognition properties, silver nanoparticles (AgNPs) are the subject of much research and have many potentials or promised applications in a variety of fields, such as electron microscopy, electronics, nanotechnology, materials science, and biomedicine. AgNPs may also have additional antimicrobial properties not found in ionic silver. FeNPs are used in MRIs, to remove impurities from water, and to deliver medications to particular parts of the body, like cancer cells [30].

2.4.3 Metallic Oxide Nanoparticles

Numerous metal oxide nanoparticles have been investigated for the electrochemical detection of biomolecules, including ZnO, NiO, MnO_2, TiO_2, Fe_2O_3, and Co_3O_4. In addition, there has been adequate emphasis on mixed metal oxides in this field. Due to their special properties, CuO-NPs are beneficial in a wide range of applications, such as catalysts, antibacterial agents, sensors, and superstrong materials. It can also come into contact and interact with other nanoparticles because of its high surface area to volume ratio. It has recently been discovered that CuO-NPs have superior antibacterial activity against *B. subtilis* and *E. coli* compared to Ag-NPs [31].

2.4.4 Lipid Based Nanoparticles

Because of their high loading capacity, low production costs, scalable manufacturing, biocompatibility, thermal and long-term stability, and ease of preparation, lipid-based nanoparticles have revolutionized therapeutic disease delivery. Specifically, during the COVID-19 pandemic, this delivery method was an essential feature of the vaccination to combat the virus. Lipid-based nanoparticles must enter target cells, release medicines, and reach the intended locations with high efficiency in order to provide successful drug delivery. To improve the therapeutic benefits, lipid-based nanoparticles' shapes and compositions can be changed to control this behaviour in vivo. Lipid-based nanoparticles are at the forefront of medication delivery and related research because of their adaptability and safety

profile. Solid lipid nanoparticles (SLNs) have a single phospholipid layer surrounding a fat-based core, ideal for carrying payloads like modRNA or RNA vaccines. Targeting molecules, such as antibodies or peptides, can also be attached to the surface for precise delivery [32].

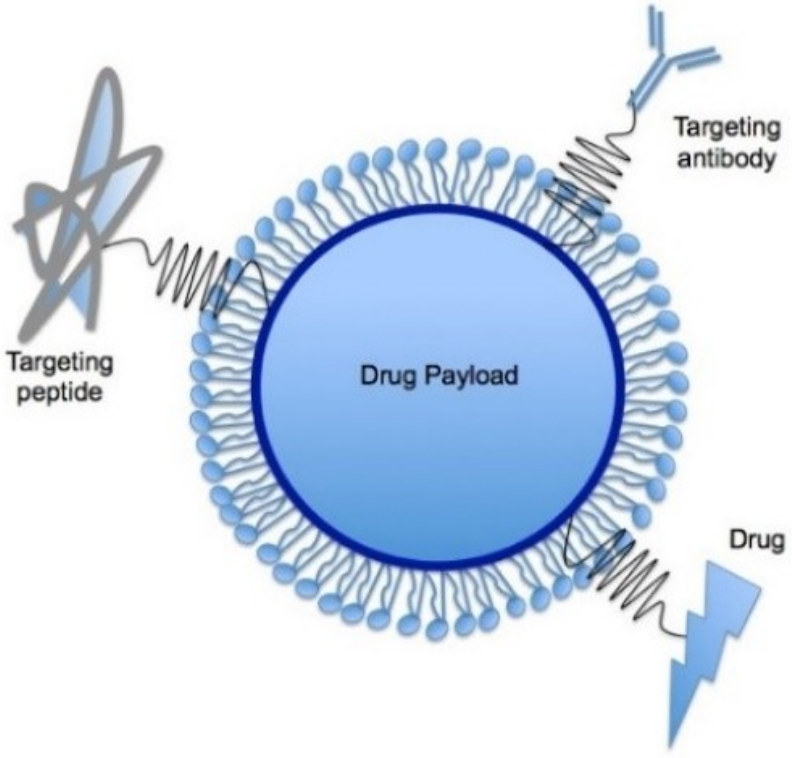

FIGURE 2.4: Solid lipid nanoparticles (SLNs) consist of a single phospholipid layer, as their core is mainly made up of lipophilic material. Therapeutic agents like modRNA, RNA vaccines, or other payloads can be loaded into the core [33].

2.4.5 Semiconductor Nanoparticles

Semiconductor nanoparticles share characteristics with metals and non-metals, which is why they have unique physical and chemical properties that make them useful for a variety of applications. One type of nanoparticle that shares characteristics with metals and non-metals is a semiconductor nanoparticle, particularly zinc sulphide (ZnS) nanoparticles, which scientists primarily study because of their excellent optical and electric properties, which include high stability, low toxicity, and the ability to generate visible light when excited by UV radiation. Semiconductor nanoparticles are used in biomedical applications for imaging and

diagnostics because of their brilliant fluorescence and ability to target specific cells or tissues [34].

2.4.6 Polymeric Nanoparticles

In the literature, these are known as polymer nanoparticles (PNPs), and they are typically organic-based NPs. Their forms are usually nano-spherical or nano-capsular. While the other molecules are adsorbed at the outer edge. Nano capsules feature a core-shell structure, with a liquid or solid core surrounded by a polymer shell that contains the active ingredient. Dendrimers are a different kind of polymeric nanoparticle. These highly branching, tree-like structures have a large number of functional groups on their surface that allow various medicinal compounds to adhere [35].

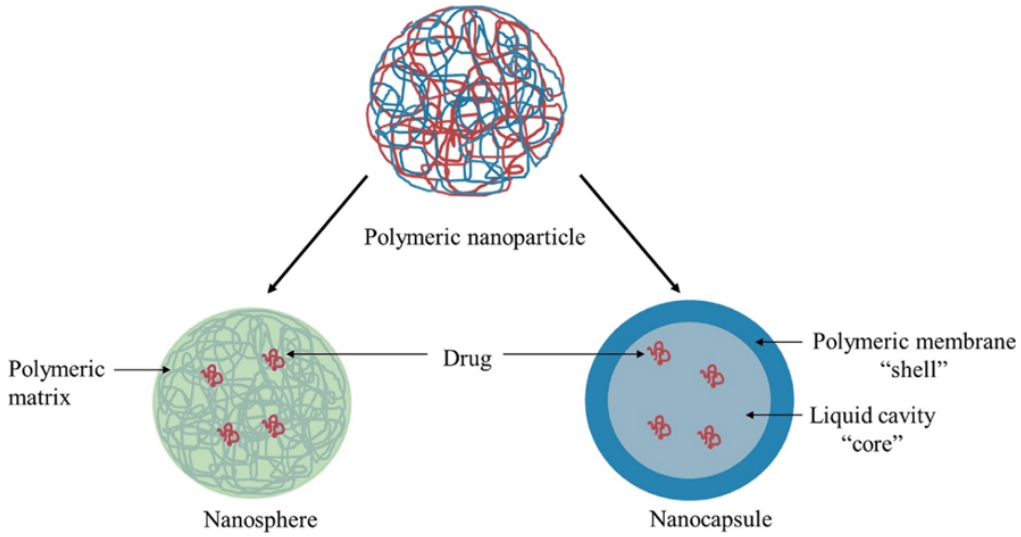

FIGURE 2.5: llustration of the two main types of nanoparticles made from polymers: solid nanospheres and hollow Nano capsules, each designed to carry and release molecules differently [36].

2.5 Biomedical Applications of Nanoparticles

Magnesium oxide nanoparticles (MgONPs) produced biogenically have special properties that make them suitable for use in environmental biotechnology and

medicine. According to reports, these biogenically produced MgONPs have antifungal, antioxidant, antibacterial, antipyretic, anti-inflammatory, and anticancer properties. Silver nanoparticle biosynthesis may produce strong antiviral drugs that limit the activities of viruses. At non-cytotoxic concentrations, silver nanoparticles have been shown to exhibit antiviral action against HIV-1. According to a study, fluconazole and silver nanoparticles together exhibited the greatest suppression of Candida albicans [37].

For medicinal purposes, ZnO-NPs are potent pharmacological agents. When compared to microparticles, ZnO-NPs appear to have a considerable therapeutic pharmacological activity. Additionally, ZnO-NPs have therapeutic properties against spores that are resistant to high temperatures and pressures [38].

2.6 Safety Concerns and Toxicity

Despite these advantages, the small size and high reactivity of nanoparticles raise concerns about potential toxicity and environmental impacts. When inhaled, ingested, or absorbed, some nanoparticles may interact with biological tissues in unanticipated ways that could have detrimental effects. Therefore, the study of nanoparticle toxicity, bioaccumulation, and environmental persistence is an essential topic of ongoing research to ensure the safe usage of these materials [39].

Immune responses can be triggered by nanoparticles, resulting in inflammation or immunological suppression that might damage tissue or increase the likelihood of autoimmune reactions. Certain nanoparticles may cause DNA damage or mutations, raising the risk of cancer, because they can disrupt normal cell division or interfere with cellular functions. In sensitive individuals, skin penetration by nanoparticles included in sunscreens and cosmetics may result in irritation, allergic reactions, or sensitisation. Furthermore, research suggests that certain nanoparticles could be able to cross the placental barrier and impact fetal development; studies on animals also suggest potential links between nanoparticle exposure and reproductive harm, reduced fertility, or developmental abnormalities [39].

2.7 Green Synthesis of Magnesium Sulfide Nanoparticles and their Biological Applications

There are very few studies regarding green synthesis of MgS nanoparticles. Green synthesized MgS from *Hordeum vulgare* successfully synthesized. The green synthesized Magnesium findings suggest that metal sulphide nanoparticles showed antibacterial action against fungus (*Aspergillus niger, Candida albicans*) and bacteria (*Staphylococcus aureus, Escherichia coli*), indicating their potential use in the fight against multidrug-resistant microorganisms.

Also, MgS-NPs from *Punica granatum* fruit extract synthesized and their activity was checked against SH-SY5Y neuroblastoma cell line [40]. However, MgS nanoparticles by *Citrus limetta* leaf extract are not reported yet. *Citrus limetta* leaf extract contains various phytochemicals flavonoids, alkaloids and tannins that are required for the synthesis of Nanoparticles [41].

2.7.1 Introduction and Medicinal Properties of *Citrus limetta* Plant

Citrus limetta plant belongs to family Rutaceae and commonly known as sweet lime. These evergreen, spiky trees range in size from small to medium, and they are native to tropical and subtropical areas of Asia, including Pakistan, China, India, Myanmar, the Philippines, Iran, and others. The fruit of the tree has a juicy endocarp, a fibrous mesocarp, and a leathery pericarp.

Citrus fruits are primarily a source of carbohydrates, including sucrose, glucose, and fructose, and have very little fat and minimal protein. Additionally, fresh citrus fruits are a good source of dietary fibre, which has been linked to decrease blood cholesterol and the avoidance of gastrointestinal disorders. The fruits provide phytochemicals such carotenoids, flavonoids, and limonoids, as well as the most abundant nutrient, vitamin C, and B vitamins (thiamin, pyridoxine, niacin,

riboflavin, pantothenic acid, and folate). These biological components are essential for improving human health because of their antioxidant qualities, capacity to be transformed into vitamin A [42]. *Citrus limetta* leaves extract also shows antimicrobial activity against various bacterial pathogens including *B. subtilis, S. aureus, K. pneumoniae* and *E. faecalis* [43].

FIGURE 2.6: *Citrus limetta* fruit and leaves [44]

Chapter 3

Methodology

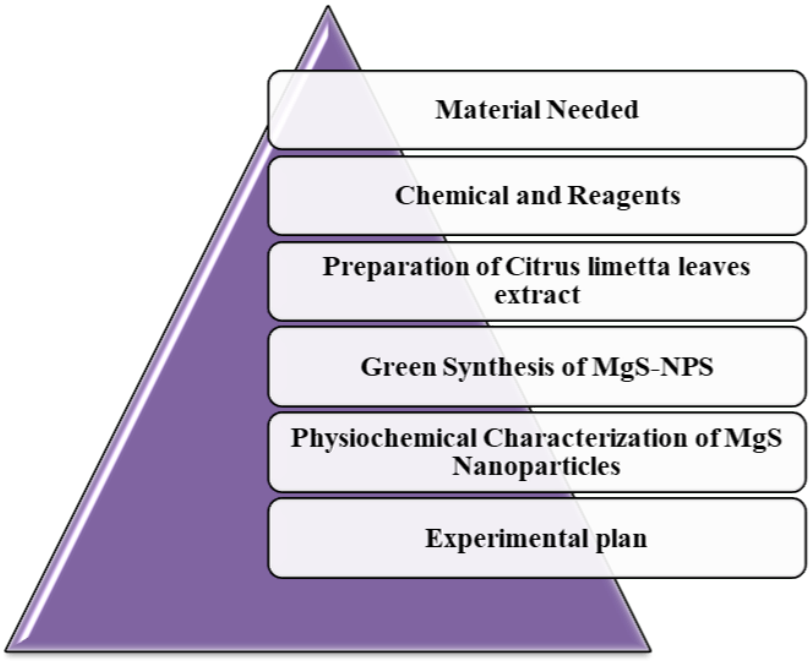

FIGURE 3.1: Research Methodology

3.1 Materials Needed

A variety of chemicals and reagents, tools and equipment, an animal model (Sprague Dawley rat), and the rat's blood and liver will all be used in this experiment.

3.2 Chemicals and Reagents

The chemicals was used in this research are Sodium sulphide (Na2S), Magnesium sulfate (MgSO4), distilled water, acetone, formalin, chloroform and magnetic stirrer.

3.3 Apparatus and Equipment

The apparatus and equipment that was used in this research are pipette Eppendorf tubes, thermometer, incubator, reaction vessels, glassware, centrifuge, beaker, magnetic stirrer, hot plate, Erlenmeyer flasks, funnels, beaker, burette, volumetric flask, graduated cylinders, calibrated digital balance, EDTA coated tubes, centrifuge machine, Falcon tubes and Culture tubes.

3.4 Methodology

The research process outlined in the study was simply categorized into four steps. Preparation of Green synthesized MgS-NPs using *Citrus limetta* leaves extract, characterization of the prepared NPs, testing of prepared Green-Synthesized MgS-NPs on rat model and assessment of different biological parameters of rat.

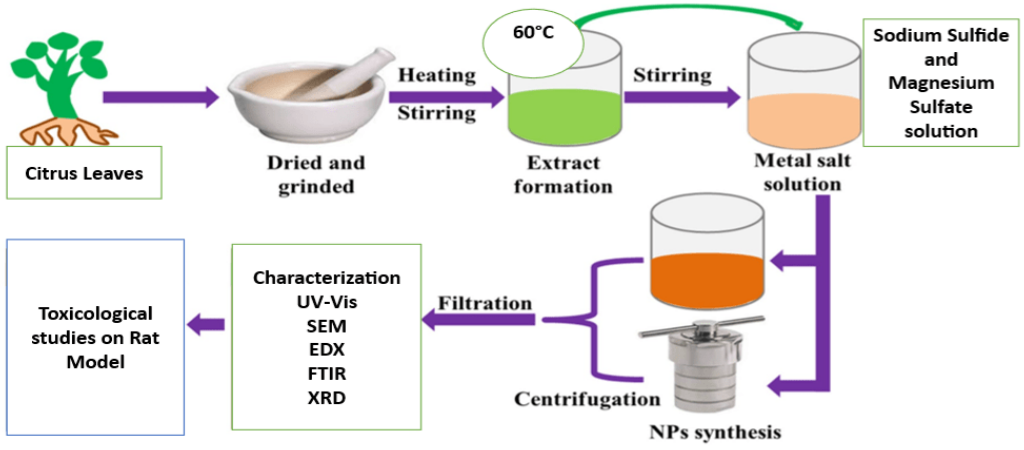

FIGURE 3.2: Overview of Methodology

3.5 Green Synthesis of MgS-NPs

3.5.1 Extract Preparation

The green synthesis of MgS-NPs was carried out using citrus limetta leaf extract. Leaves were collected from surroundings of Islamabad. Leaves and fruit were identified and authenticated by Botany department Arid Agriculture University, Rawalpindi.

To prepare the extract, 10 grams of the dried leaf powder was mixed with 120 mL distilled water, heated at 60 ^{o}C for 2 hours. The mixture in the flask was the transferred to shaking incubator for the next 24 hrs., followed by filtration and drying of the crude extract at 45 ^{o}C for 12 hrs. After drying the extract was collected in a vial and was utilized for synthesis of MgS-NPs.

FIGURE 3.3: *Citrus limetta* leaves washed, dried and chopped. Then added into distilled water.

3.5.2 Synthesis of MgS-NPs

The synthesis of green synthesized MgS-NPs involved the utilization of specific amounts of precursor, reducing and capping materials. Primarily, 0.125 M of $MgSO_4.7\,H_2O$ (1.50 g), 0.125 M of Na_2S (1.5 g), and plant extract (100 mg) were prepared separately in 100 mL distilled water. Subsequently, the prepared solutions of$MgSO_4.7\,H_2O$ and Na4S were mixed and kept on stirring for 10 min. Later on, the plant extract solution was added to the previously prepared mixture. Slight color changes were observed as the solution was placed on the magnetic stirrer for 4h at 65 ^oC. Conclusively, the slurry was collected and washed three times using a centrifuge at 6000 rpm for 8 min for each step of collection and washing with distilled water to improve the purity of nanoparticles. The materials were then placed in a drying oven in a clean petri plate at 75 ^oC, and the finished dried product was collected after 20 h. Following on, the material was grounded into fine powder in pestle and mortar and calcination was performed at 100 ^oC for 2 h to get the MgS-NPs. Finally, the prepared materials were stored at room temperature and were further subjected to characterization analysis and biological properties.

3.6 MgS Nanoparticles Physicochemical Characterization

To better understand the properties of the synthesized MgS nanoparticles, several techniques was used, including UV-Visible (UV-Vis) Spectroscopy, Fourier Transform Infrared Spectroscopy (FTIR), Scanning Electron Microscopy (SEM), Energy-Dispersive X-ray Spectroscopy (EDX), and X-ray Diffraction (XRD) [45].

3.6.1 FTIR Spectroscopy

FTIR, which stands for *Fourier Transform Infrared Spectroscopy*, is like a chemical detective tool for nanoparticles. Nanoparticles, being so tiny, have a very distinct

surface chemistry compared to bulk materials. Imagine them like little puzzle pieces, and the surface of these pieces has various "functional groups" things like hydroxyl groups (-OH), carboxyl groups (-COOH), or amine groups (-NH2). These groups play a big role in how nanoparticles interact with their surroundings, like how they bond with other molecules, or how they react in a chemical process [46].

Now, FTIR comes in as the magnifying glass for these chemical groups. When a nanoparticle sample is exposed to infrared light, the different chemical bonds in those functional groups will absorb specific frequencies of light. This gives you a unique "fingerprint" for each type of bond.

So, FTIR can tell you exactly what kinds of chemical groups are present on the surface of the nanoparticles.In essence, using FTIR is like getting a chemical snapshot of the nanoparticle's surface, which helps scientists understand how these particles might behave in real world applica- tions whether it's for drug delivery, catalysis, or even in environmental monitoring [47].

3.6.2 UV-Visible (UV-vis) Spectroscopy

UV-Visible spectroscopy was used as the first step to analyze the synthesized magnesium sulfide (MgS) nanoparticles. This technique measures how the sample absorbs light in the ultraviolet and visible range, offering insight into the material's electronic transitions. By observing specific absorption peaks, we can confirm the presence of MgS and determine whether the nanoparticles have successfully formed. Each material has a unique absorption pattern, so the appearance of characteristic peaks serves as an initial fingerprint of successful synthesis.

Beyond simply detecting the nanoparticles, UV-Vis spectroscopy also allows us to estimate their concentration and gain clues about particle size or aggregation through shifts in absorption. It's a quick, non-destructive method that provides both qualitative and quantitative information, making it an ideal starting point before moving on to more advanced techniques [48].

3.6.3 X-Ray Diffraction (XRD)

X-ray diffraction was used to determine whether the synthesized MgS nanoparticles are crystalline in nature. This technique works by directing X-rays at the sample and analyzing the way they scatter, producing a pattern that reveals the internal atomic structure. If the nanoparticles are crystalline, they will generate distinct peaks in the diffraction pattern, which can then be matched to known MgS structures. This allows us to not only confirm their formation but also verify their crystallinity an important property that can influence their physical and chemical behavior.

In addition to identifying crystallinity, XRD is also valuable for assessing the purity of the sample. Impurities or unwanted by-products will typically produce extra peaks or cause noticeable changes in the diffraction pattern. By carefully analyzing these patterns, we can ensure that the synthesized material is primarily composed of pure MgS and not contaminated with other phases [49].

3.6.4 Scanning Electron Microscopy (SEM)

Scanning Electron Microscopy (SEM) was used to closely examine the surface and structure of the MgS nanoparticles. This technique produces highly detailed images by scanning the sample with a focused beam of electrons, allowing us to directly see what the particles look like. Unlike other methods that give indirect data, SEM lets us visually confirm the shape, surface features, and overall appearance of the nanoparticles. It's a powerful way to explore how the particles were formed and how they behave at the microscopic level.

In addition to capturing the particles' shape, SEM helps measure their size and check for consistency across the sample. We can evaluate whether the nanoparticles are evenly sized, if they've clumped together, or if they display irregularities. This information is important for understanding how successful and controlled the synthesis process was. By providing clear, magnified images, SEM gives us a

visual confirmation of the material's physical characteristics, making it easier to assess the quality and uniformity of the final product [50].

3.6.5 Energy-Dispersive X-ray Spectroscopy (EDX)

Energy-Dispersive X-ray Spectroscopy (EDX), often used alongside SEM, was employed to identify the elements present in the MgS nanoparticles. When the electron beam hits the sample, it causes the atoms within to emit X-rays at energies unique to each element.

By analyzing these signals, EDX can tell us exactly which elements are present in the nanoparticles and in what relative amounts. This is especially useful for confirming that magnesium and sulfur are the main components, as expected.

EDX also plays a crucial role in checking for impurities. Sometimes, during the synthesis process, unwanted elements like oxygen or carbon can be introduced either from the environment or from leftover chemicals. EDX can detect even small amounts of these contaminants, helping us evaluate the overall purity of the sample. In this way, EDX not only verifies the composition of the nanoparticles but also ensures the quality and cleanliness of the final product [51].

3.7 Experimental Plan

This study was conducted over a 20 day period in a carefully monitored and controlled animal research facility. The aim is to evaluate the effects of magnesium sulfide (MgS) nanoparticles using a straightforward, three group experimental design to ensure clarity and reproducibility of the results.

3.7.1 Animal Selection

The experiment will involve healthy adult male Sprague Dawley rats, known for their docile nature and widespread use in laboratory studies. Each rat will weigh

between 150 and 200 grams and be aged between six to eight weeks to ensure uniformity and maturity. They was housed in a clean, pathogen-free animal facility where environmental conditions such as temperature, humidity, and light cycles (12-hour light/dark) are carefully regulated. These controlled settings help maintain the well-being of the animals and ensure that external factors do not interfere with the experimental outcomes [52].

3.7.2 Acclimatization

Before the start of the experiment, all rats will undergo a one-week acclimatization period. This allows the animals time to adjust to their new environment, handling routines, and daily care. Acclimatization is a critical step in animal studies as it helps reduce stress, stabilize physiological responses, and minimize variability in the data. This period ensures that when the experiment begins, the rats are in a stable condition, which leads to more reliable and consistent results.

3.7.3 Experimental Groups

A total of nine rats was randomly assigned to one of three experimental groups, with three rats in each group:

Group 1 (Control) This group will serve as the baseline for comparison. Rats in this group will receive only a standard laboratory diet and purified water for 20 days, with no exposure to MgS nanoparticles.

Group 2 (Low Dose) These rats will receive a low dose of magnesium sulfide (MgS) nanoparticles along with the same regular diet and purified water for 20 days.

Group 3 (High Dose) This group was given a higher dose of MgS nanopar- ticles, again with a standard diet and purified water, for the same 20-day period.

This group design allows the study to assess the biological impact of different MgS nanoparticle concentrations and identify any dose-dependent effects.

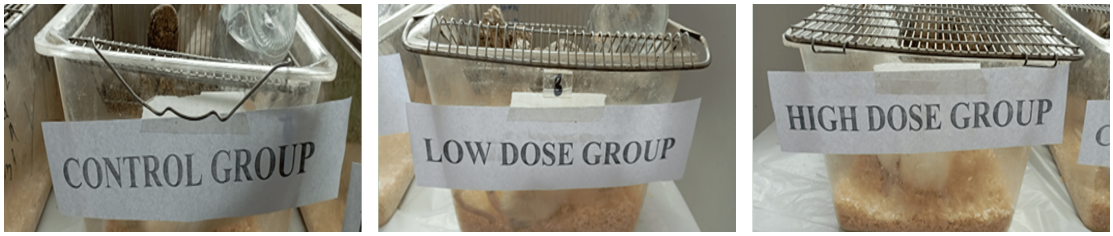

FIGURE 3.4: Sprague Dawley rats categorized into three groups

3.7.4 Dosage Optimization

The average weight of the rat was 200gm. Dose preparation of MgS-NPs was decided on the basis of tolerate dose of CuS NPs which was 8.66 mg/kg. On the basis of tolerate dose the dosage was decided as 1.73 mg/200gm (low dose taking group) and 3.46mg/200gm (high dose taking group) [53].

FIGURE 3.5: Rat being given dose using feeding tube

3.7.5 Morphological Assay

To monitor physical health and potential changes during treatment, the body weight and general behavior of each rat was recorded after every five days. An electronic weighing scale was used for accuracy. Observing weight gain or loss, as well as any behavioral changes, can help indicate the biological response to MgS exposure and provide early signs of toxicity or stress.

3.7.6 Animal Dissection

On the 21^{st} day, the rats was ethically euthanized to collect tissue samples for further analysis. Each animal will first be deeply anesthetized with pentobarbitone sodium (50 mg/kg) to ensure they feel no pain. Once fully anesthetized, euthanasia was performed via cervical dislocation. Liver tissues will then be carefully extracted and either preserved in 10% formalin for histological examination or snap-frozen in liquid nitrogen for biochemical and molecular studies. All samples was stored at -70°C to maintain their integrity until analysis [54].

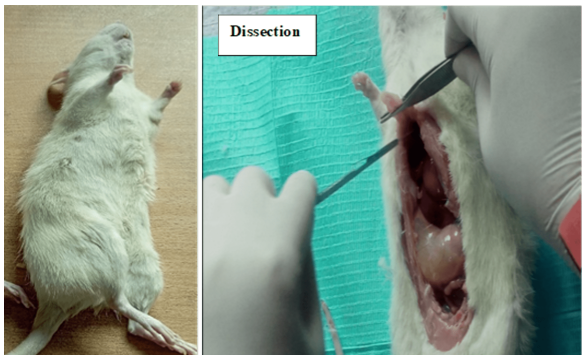

FIGURE 3.6: Rat being anesthetized and dissected

3.7.7 Biochemical Assay

While the rats are under anesthesia, blood samples was collected via cardiac puncture. These samples was stored at –20oC and later analyzed for key biochemical markers. Tests will include liver function tests (such as ALT and AST) and RFT [55].

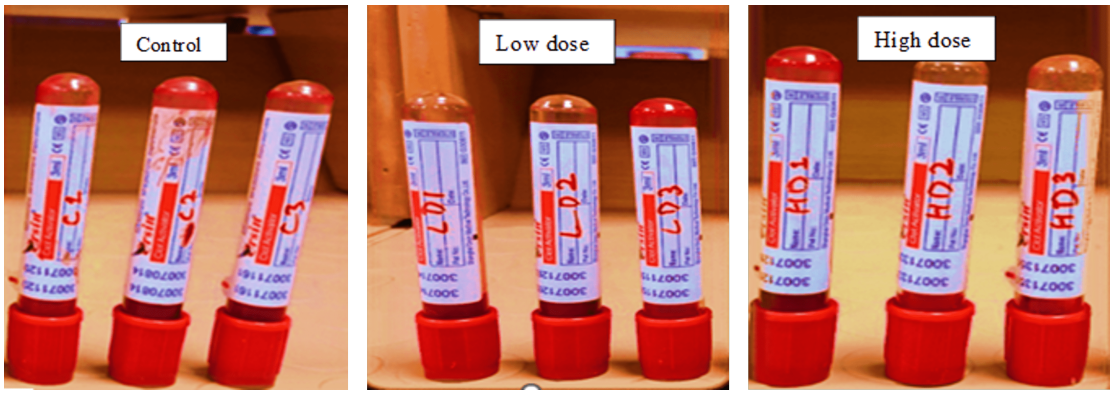

FIGURE 3.7: Blood sample for biochemical analysis

3.7.8 Hematological Analysis

The parameters that were checked in after hematological analysis were: red blood cells (RBC), white blood cells (WBC), platelets/thrombocytes (PLT), hemoglobin (Hb), Hematocrit (HCT), mean corpuscular volume (MCV), mean corpuscular hemoglobin concentration (MCHC), lymphocytes (LYMPHO), monocytes (MONO), eosinophils (EOS), and neutrophils (NEU), mean corpuscular hemoglobin (MCH) [56].

FIGURE 3.8: Blood sample for biochemical analysis

3.7.9 Histopathological Analysis

After the treatment period, the liver and intestines was collected from each rat for detailed microscopic analysis. The tissues was fixed in 10% formalin, embedded in paraffin wax, sectioned into thin slices, and stained using hematoxylin and eosin (H&E). This staining technique allows researchers to closely examine cellular structures and detect any abnormalities such as tissue damage, inflammation, or necrosis that may have resulted from the MgS nanoparticle exposure [57].

3.7.10 Statistical Analysis

To determine whether any differences between groups are statistically significant, a one-way Analysis of Variance (ANOVA) was used [58].

Chapter 4

Results

4.1 Preparation of *Citrus limetta* Leaves Extract and MgS-NPs Synthesis

Extract was prepared from leaves in 120 ml of distilled water after heating followed by filtration results in yellowish light green color solution. 0.1 M solution of MgSO4 and Na2S were prepared in 100 ml distilled water and then mixed along with stirring. Solution then added dropwise into extract for 4h and then giving centrifugation along with washing. Bioactive compunds like polyphenols and flavonoids act as reducing agents and color of the solution changes to pale yellow which indicates the synthesis of MgS nanoparticles [59]. Nanoparticles then dried and stored for characterization and further application.

FIGURE 4.1: Green Synthesized MgS-NPs after washing and drying

4.2 Characterization of Green Synthesized MgS Nanoparticles

4.3 SEM-EDX

SEM (Scanning Electron Microscopy) was done to identify the morphology and size of the synthesized nanoparticles and EDX (Energy Dispersive X-Ray) was also performed to confirm the elemental composition of Magnesium Sulfide NPs synthesized by Citrus limetta leaf extract.

According to SEM, the size of nanoparticles is between 80-100nm, Image formed by SEM is shown in Figure below which demonstrate the formation of MgS-NPs in crystalline form flake like lamellar sheets at different resolutions. Particles show a tendency to form clusters or agglomerates, which is typical for metal sulfide nanoparticles.

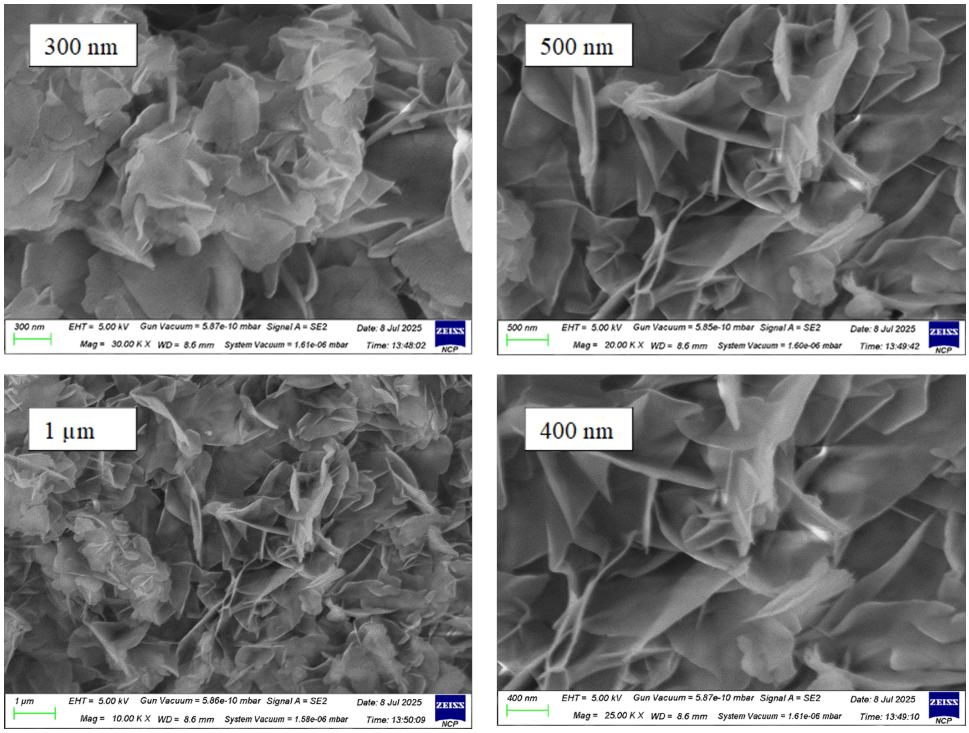

FIGURE 4.2: SEM images of MgS nanoparticles at different resolutions

EDX analysis of green synthesized MgS-NPs is presented in the form of different peaks. The elemental analysis showed atomic and mass percentages of O, Mg, C,

S, Na and Cl. Na, C and Cl must have adhered from the Citrus limetta leaves extract and Mg is present at highest percentage in different spectra, in spectra 6 and 7 Mg % is 27.3% and 29.6%, which shows the purity of NPs. Also traces of Au are present mainly because gold is coated over non-conductive samples like MgS nanoparticles to improve image quality and reduced charging during SEM imaging.

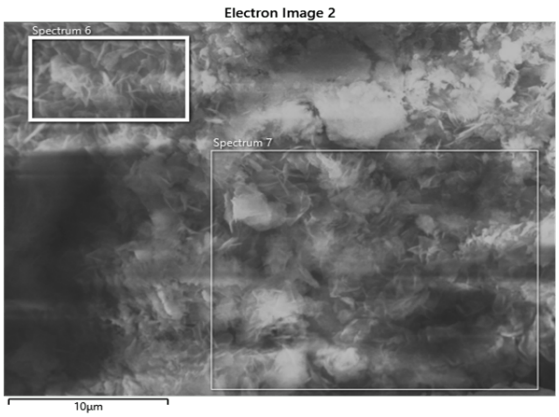

FIGURE 4.3: SEM of MgS-NPs at 10 microns

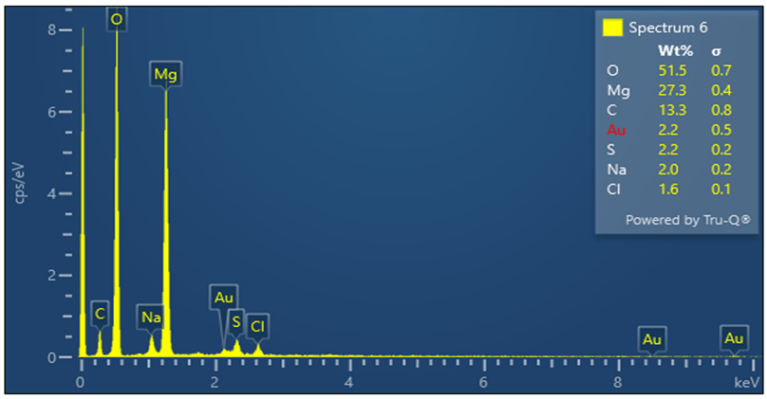

FIGURE 4.4: EDX Spectra 6 of green synthesized MgS Nanoparticles

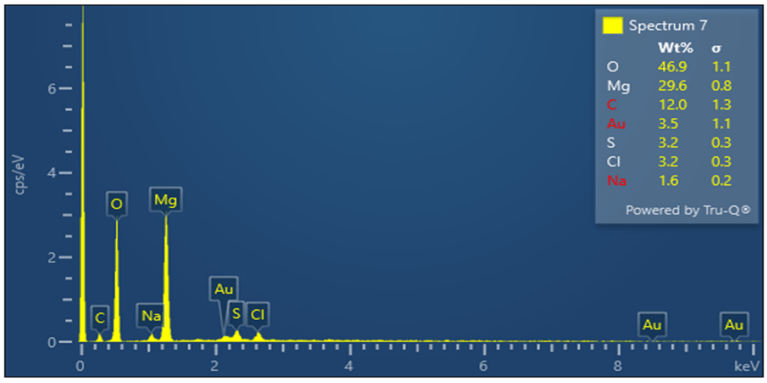

FIGURE 4.5: EDX Spectra 7 of green synthesized MgS-NPs

4.3.1 UV-Vis Spectroscopy

Because of its cost and ease of use, this approach is frequently employed in a wide range of theoretical and practical applications. MgS-NPs UV-visible absorption spectra, which were derived from Citrus limetta leaves extract, were measured at room temperature using a Genesys 10S UV-Vis apparatus. By combining the NP solution with distilled water, the spectral response (SPR) of the nanoparticles (NP) was determined in the 200–800 nm range. MgS Uv-Vis absorption was reported around 280-320nm range. MgS nanoparticles show absorption peaks around 260-320 nm. Green synthesized MgS-NPs showed highest peak at 300nm which confirms the existence of MgS nanoparticles [60].

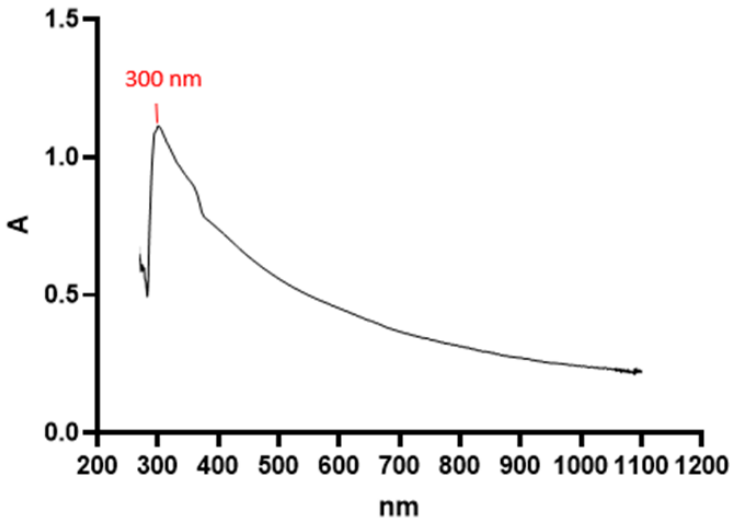

FIGURE 4.6: Uv-Vis Analysis of Green synthesized MgS Nanoparticles

4.3.2 FTIR Analysis

The FTIR analysis of MgS nanoparticles from Citrus limetta leaves extract reveals several functional groups, particularly **hydroxyl, carbonyl/ether/amine**, and **aromatic compounds** which play a pivotal role in the green synthesis of MgS nanoparticles [61]. These groups act as natural *reducing and stabilizing agents*, confirming the bio-fabrication of MgS through peaks observed at **3672, 1244, 1055, 881, 658, and 511** cm^{-1}.

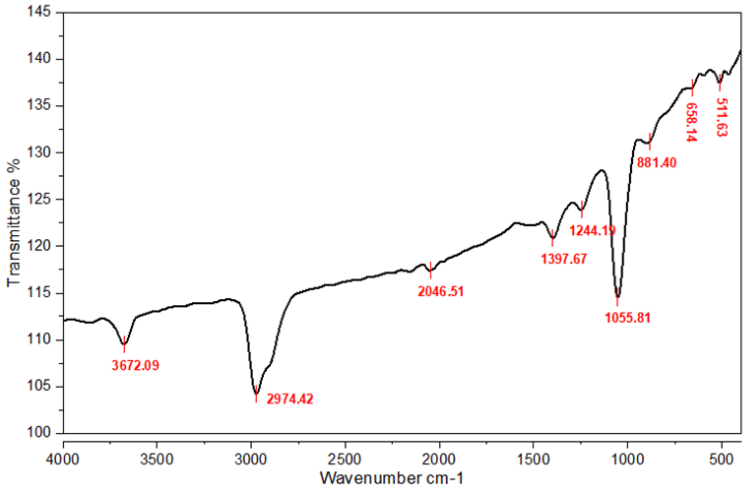

FIGURE 4.7: Interpretation of various peaks in FTIR analysis of MgS-Nps from Citrus limetta leaves extract

TABLE 4.1: Interpretation of various peaks in FTIR analysis of MgS-Nps from Citrus limetta leaves extract

FTIR Peak (cm^{-1})	**Functional Group**	**Significance in MgS NP Synthesis**
3672	Hydroxyl (–OH) group (alcohols, phenols)	Acts as a reducing agent to convert Mg^{2+} and S^{2-} into MgS. Also stabilizes NPs by hydrogen bonding.
2974	Alkyl C–H stretch	Provides hydrophobic environment for capping and nanoparticle stabilization.
1244 & 1055	C–O / C–N (esters, ethers, amines)	Play a dual role: reduce metal ions and bind/cap NPs to prevent agglomeration.
881	C=C out-of-plane bending (alkenes/aromatics)	Aromatic π-electron systems facilitate electron donation to metal ions.
658	C–Cl or halogen group vibrations	May contribute to surface modification
511	Metal–S vibrations	Indicates successful formation of metal-based nanoparticles like MgS.
3672	Hydroxyl (–OH) group (alcohols, phenols)	Acts as a reducing agent to convert Mg^{2+} and S^{2-} into Mg S. Also stabilizes NPs by hydrogen bonding.
2974	Alkyl C–H stretch	Provides hydrophobic environment for capping and nanoparticle stabilization.

4.3.3 XRD

In the context of magnesium sulfide (MgS) nanoparticles, XRD plays a pivotal role in validating the crystalline phase formed during synthesis. Since MgS can exist in multiple polymorphs, such as cubic or hexagonal structures, XRD helps to distinguish between them based on their unique peak positions in the diffraction pattern. Moreover, XRD is used to confirm the purity of the synthesized nanoparticles by identifying and eliminating any unwanted phases like magnesium oxide (MgO), magnesium sulfate ($MgSO_4$), or other impurities. This is especially important in green synthesis methods where plant extracts may introduce additional organic or inorganic components [62].

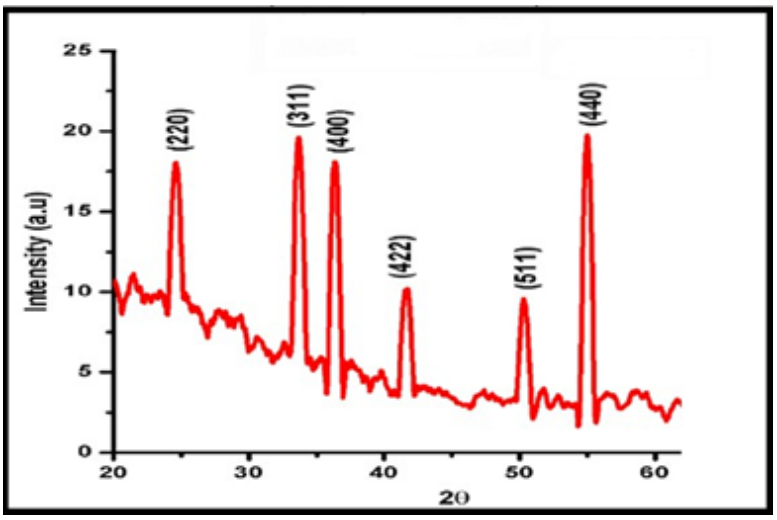

FIGURE 4.8: X-ray diffraction pattern of MgS-NPs

The image depicts an X-ray diffraction pattern of Magnesium Sulfide nanoparticles (NPs), as shown in Fig. 2. The graph shows the intensity (in arbitrary units) on the y-axis and the diffraction angle (2θ) on the x-axis, ranging from 5^o to 85^o. The most prominent peak is located around 45^o, corresponding to the (220) crystallographic plane of the MgS-NPs. The XRD pattern indicates a crystalline structure, with the sharp peak suggesting well-defined crystallinity. The rest of the graph shows a decrease in intensity as the angle increases, implying fewer or no detectable crystallographic planes beyond the identified peak. This pattern can be used to study the structural properties of the MgS-NPs and confirm their

phase purity and particle size, important for their applications in various fields like catalysis, electronics, and materials science.

4.4 Body Weight of Rats

Over the course of 20 days, the rats' body weights in three groups—control, low dosage, and high dose were recorded [63]. The body weight of the control group increased steadily from 165 ± 25 g on day 1 to 206 ± 15.09 g on day 20. In a similar way, the low-dose group showed weight increasing gradually from 178 ± 2 g to 206 ± 4 g.

The high-dose group, on the other hand, started with a lower baseline weight (150 ± 16 g) and increased more slowly, reaching 195 ± 4.5 g by day 20.

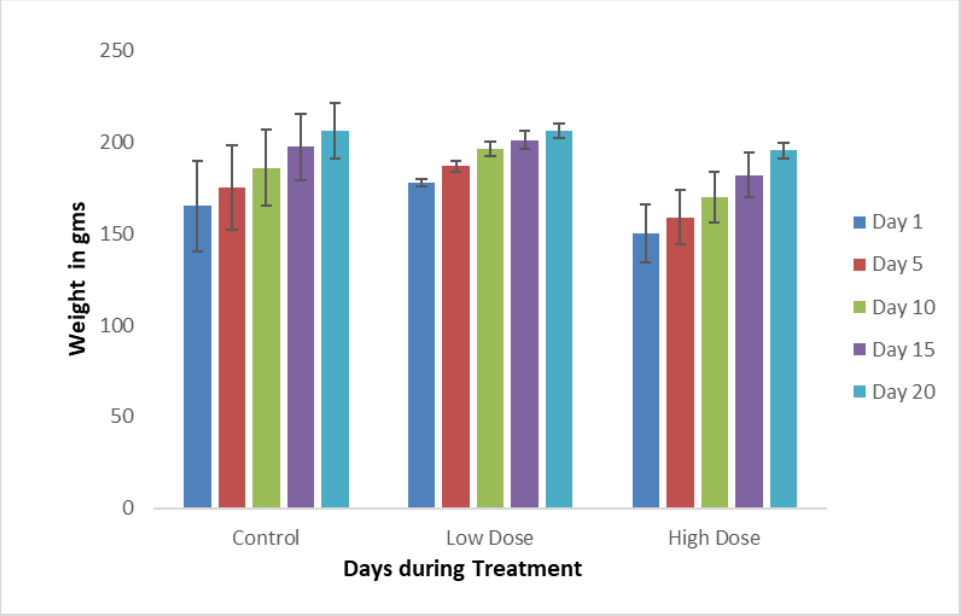

FIGURE 4.9: Body weight of rats from day 1 to day 20. one way ANOVA along Mean±SD when p-value was <0.05

Over time, all groups gained weight, although the rate and amount of increase varied greatly, especially between the high-dose and low-dose groups. The observed variations in weight increase between the groups are statistically significant, as indicated by the p-value of less than 0.05. This suggests that the medication,

particularly at higher dosages, may have had an adverse effect on metabolism or body weight control.

TABLE 4.2: Low dose and high dose group weight measurements in comparison with control group in one way ANOVA along Mean±SD when p-value was <0.05

Group	**1st Day**	**5th Day**	**10th Day**	**15th Day**	**20th Day**
control	165±25	175± 23	186± 20.5	197.3± 18.1	206± 15.09
low dose	178± 2	187± 3	196± 4	201± 5	206± 4
high dose	150± 16	159.33± 15.50	170± 14	182 ± 12	195± 4.50

4.5 Hematological Analysis

4.5.1 HB

A vital component of oxygen transport, hemoglobin (Hb) is also a crucial marker of haematological and general physiological health [64]. In this investigation, the control group's mean hemoglobin level was 13 ± 0.818 g/dL, but the low-dose and high-dose groups' levels were marginally lower at 12.56 ± 0.305 g/dL and 12.06 ± 0.251 g/dL, respectively.

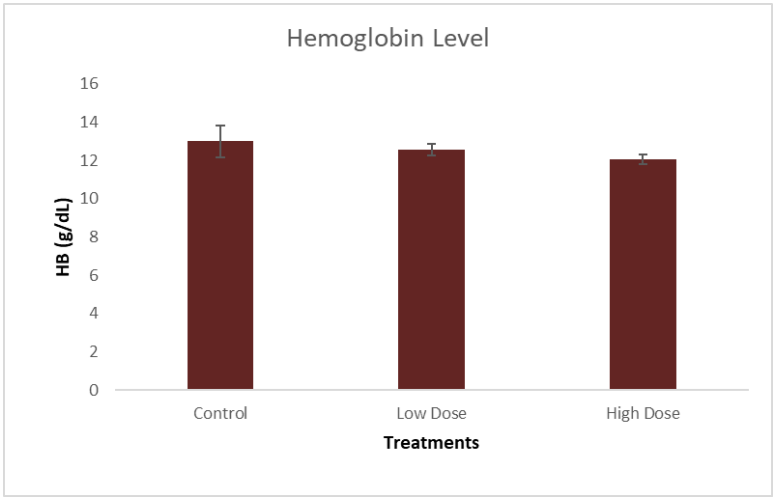

FIGURE 4.10: Body weight of rats from day 1 to day 20. one way ANOVA along Mean±SD when p-value was <0.05

The p-value of 0.173 suggests that the differences are not statistically significant, even with this slight drop. This implies that the therapy had no discernible effect

on hemoglobin concentration over the research period, even at increasing dosages. Given that the Hb levels were comparatively constant across all groups, the substance may be deemed hematologically safe at the studied doses since it is probably not harmful to the generation of red blood cells or erythropoietic function.

TABLE 4.3: Mean±SD values for HB of all groups compared by one-way ANOVA

Parameter	Control	Low Dose	High Dose	P value
HB	13± 0.818	12.56 ± 0.305	12.06± 0.251	0.173

4.5.2 RBCs

The movement of oxygen from the lungs to bodily tissues and the elimination of carbon dioxide depend on red blood cells, or RBCs. Anemia, bone marrow suppression, or systemic toxicity may be indicated by any notable decrease in their count, which is an essential indicator of blood health [65].

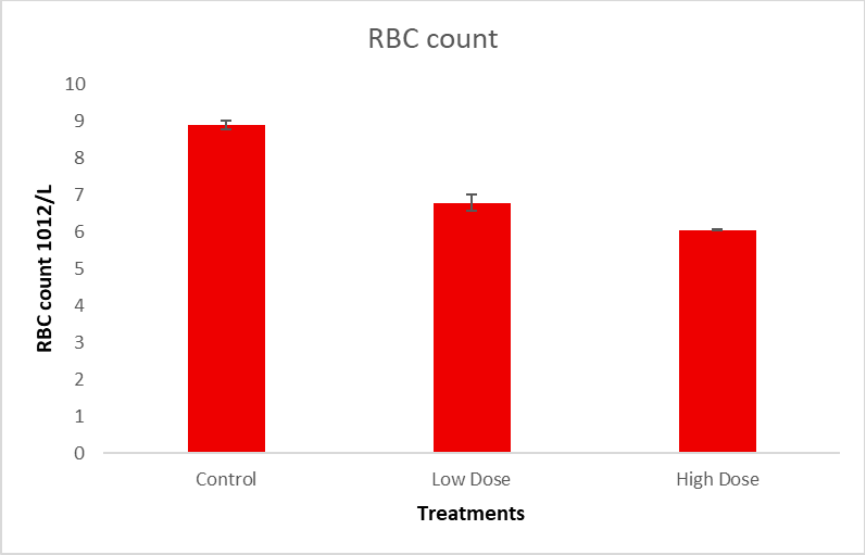

FIGURE 4.11: RBCs (mil/mm3) of all Groups

In this study, the control group maintained a normal RBC count of 8.89 ± 0.12 million/μL, while the low-dose and high-dose groups showed a significant reduction to 6.78 ± 0.225 and 6.04 ± 0.015 million/μL, respectively. The associated p-value of 0.002 confirms that these differences are statistically significant.

TABLE 4.4: Mean±SD values for RBCs of all groups compared by one-way ANOVA

Parameter	Control	Low Dose	High Dose	P value
RBCs	8.89± 0.12	6.78± 0.225	6.04± 0.015	0.002

4.5.3 WBCs

White blood cells, or WBCs, are essential parts of the immune system that help protect the body against foreign substances, inflammation, and diseases. WBC counts that are elevated or decreased may indicate pathological or physiological alterations, such as immune suppression or activation [66].

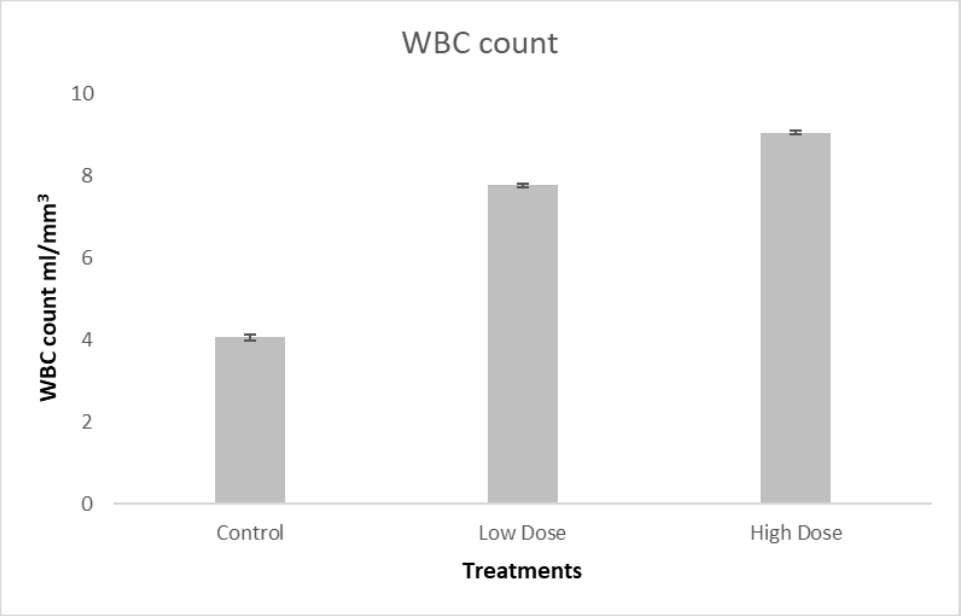

FIGURE 4.12: Graph showing WBCs (mil/mm3) in all groups

In this study, the control group exhibited a normal WBC count of 4.05 ± 0.085 while the low-dose group showed a significant increase to 7.76 ± 0.03, and the high-dose group further elevated to 9.05 ± 0.04. The p-value of 0.0003 indicates that these differences are highly statistically significant.

This substantial and dose-dependent increase in WBCs suggests that the administered compound may have stimulated an immune response or induced mild systemic inflammation, particularly at higher doses.

TABLE 4.5: Mean±SD values for WBCs of all groups compared by one-way ANOVA

Parameter	Control	Low Dose	High Dose	P value
WBCs	4.05±0.085	7.76± 0.03	9.05± 0.04	0.0003

4.5.4 Platelets

Platelets (thrombocytes) are small blood components essential for clot formation and preventing bleeding. Normal platelet levels are crucial for vascular integrity and immune defense. Abnormal counts can lead to bleeding or clotting disorders. In this study, platelet counts decreased significantly with higher doses [67]. The control group had 361 ± 47.4, the low-dose group 355 ± 17, and the high-dose group 229 ± 17. A P value of 0.003 indicates a significant, dose-dependent reduction in platelet levels.

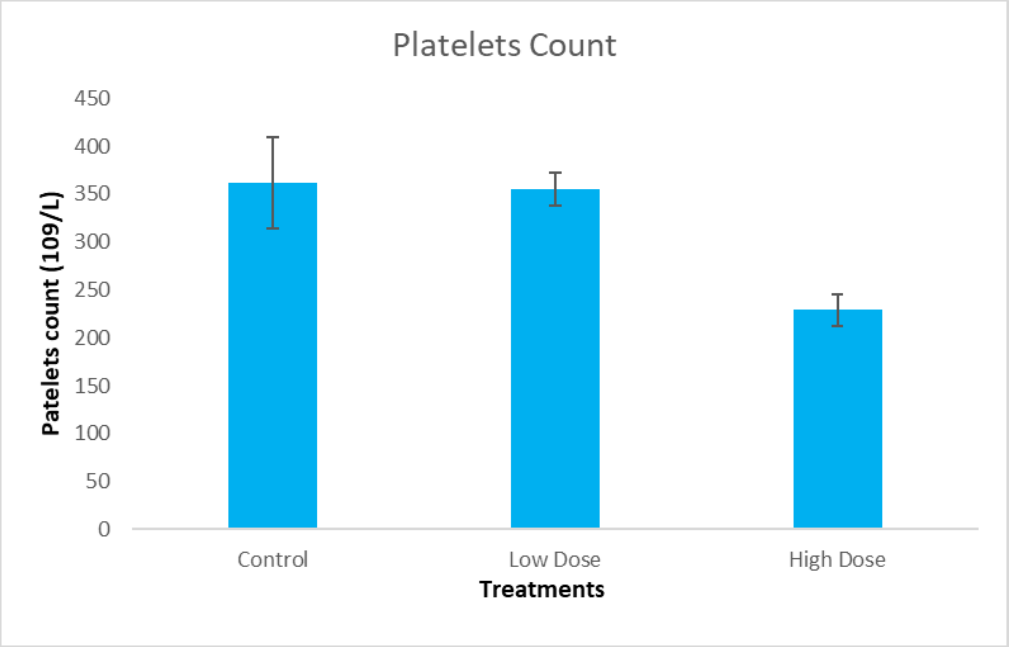

FIGURE 4.13: Graphical representation of Platelets Count

TABLE 4.6: Mean±SD values of Platelets count for all groups compared by one way ANOVA

Parameter	Control	Low Dose	High Dose	P value
Platelets	361±47.4	355±17	229±17	0.003

4.5.5 Neutrophils

Neutrophils are the most abundant type of white blood cells and play a key role in the body's defense against infections, particularly bacterial and fungal pathogens. They are essential components of the innate immune response. In this study, neutrophil counts showed a significant dose-dependent decrease [68]. The control group had 36.96 ± 1.379, while the low-dose group dropped to 10.16 ± 0.351, and the high-dose group further declined to 7.1 ± 0.3. The P value of 0.0001 indicates this reduction is highly significant, suggesting that higher doses may suppress neutrophil levels and potentially impair immune function.

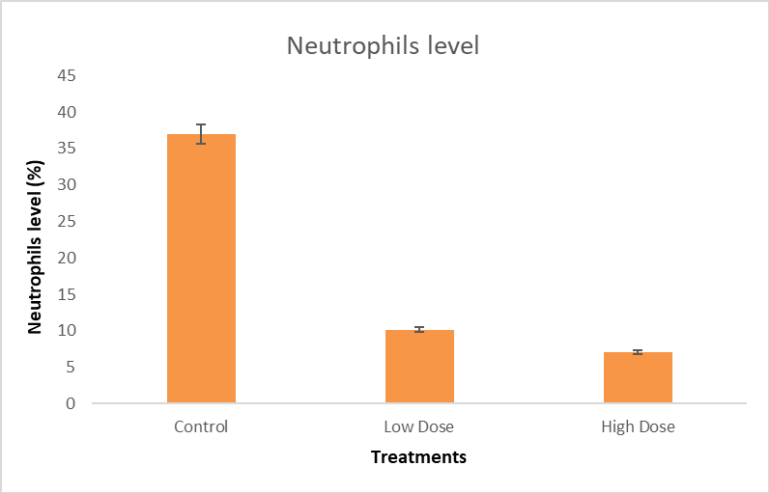

FIGURE 4.14: Neutrophils level (%) of all groups, when p value was <0.05

TABLE 4.7: Mean±SD values of Neutrophil count for all groups compared by one way ANOVA

Parameter	Control	Low Dose	High Dose	P value
Neutrophils	36.96±1.379	10.16±0.351	7.1±0.3	0.0001

4.5.6 Lymphocytes

Lymphocytes are a type of white blood cell essential for adaptive immunity, including the production of antibodies and coordination of immune responses. They play a vital role in defending the body against viral infections and in immune regulation. In this study, lymphocyte levels increased significantly with higher doses

[69]. The control group had 54.1 ± 3.99, the low-dose group rose to 69.3 ± 1.87, and the high-dose group reached 80.33 ± 2.51. The P value of 0.001 indicates a statistically significant, dose-dependent increase, suggesting a potential stimulatory effect on lymphocyte production or activity.

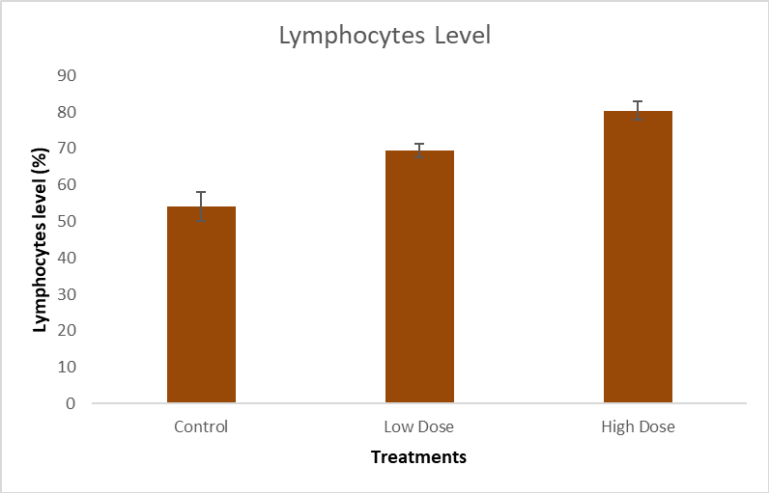

FIGURE 4.15: Lymphocytes level (%) of all groups, when p value was <0.05

TABLE 4.8: Mean±SD values of Neutrophil count for all groups compared by one way ANOVA

Parameter	Control	Low Dose	High Dose	P value
Lymphocytes	54.1±3.99	69.3±1.87	80.33±2.51	0.001

4.5.7 Monocytes

Monocytes are white blood cells involved in immune defense, particularly in phagocytosis, inflammation, and antigen presentation. Their levels in blood can indicate immune activation or suppression, depending on physiological or pathological conditions [70]. The table shows a significant change in monocyte levels across treatment groups (P = 0). The low dose group exhibited a substantial increase (11.03 ± 0.15) compared to control (4.5 ± 0.81), indicating a strong immune response. Interestingly, the high dose group showed a reduced level (7.13 ± 0.25) relative to the low dose, suggesting a possible immunomodulatory or suppressive effect at higher concentrations. This dose-dependent trend highlights the treatment's impact on immune function.

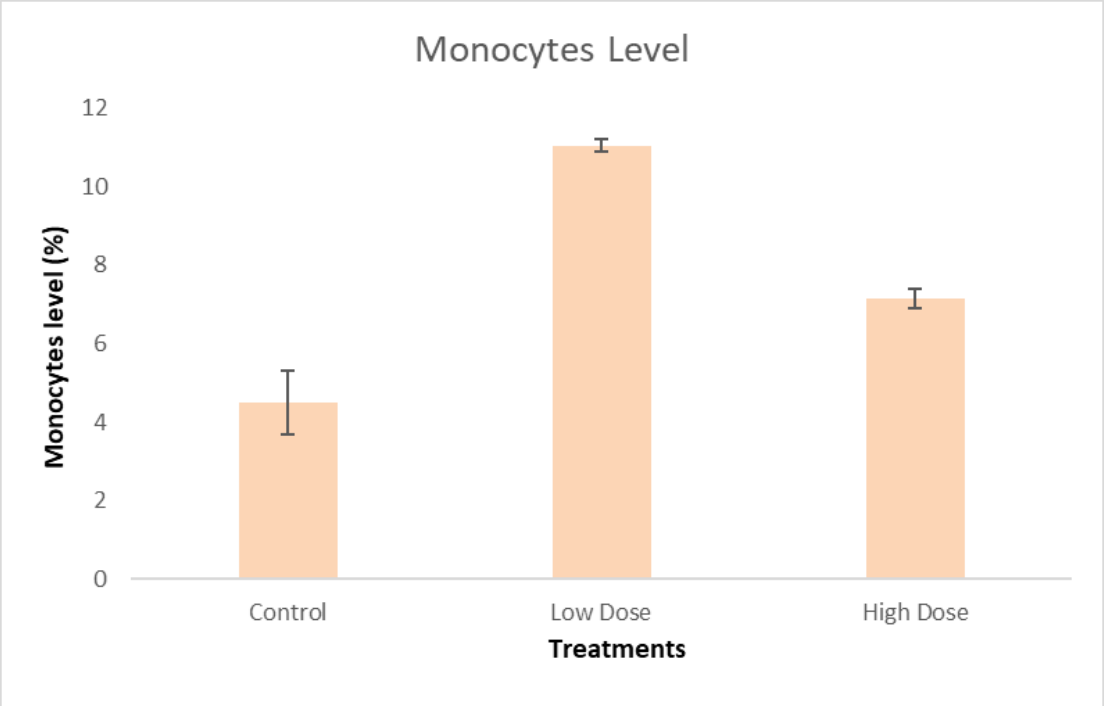

FIGURE 4.16: Graphical presentation of Monocytes level (%) of all groups

TABLE 4.9: Mean±SD values of Monocytes count for all groups compared by one way ANOVA

Parameter	Control	Low Dose	High Dose	P value
Monocytes	4.5±0.81	11.03±0.15	7.13±0.25	0

4.5.8 Eosinophils

Eosinophils are a type of white blood cell primarily involved in allergic responses and defense against parasitic infections. Changes in eosinophil levels can indicate allergic reactions, parasitic infestations, or immune system modulation [71]. In the table, eosinophil levels show a statistically significant difference across groups ($P = 0.0008$).

The low dose group shows a slight increase (7.2 ± 0.2) compared to the control (6.46 ± 0.55), suggesting mild activation. In contrast, the high dose group displays a notable decrease (5.1 ± 0.1), indicating a potential suppressive effect at higher concentrations. This suggests a dose-dependent immunomodulatory effect on eosinophils.

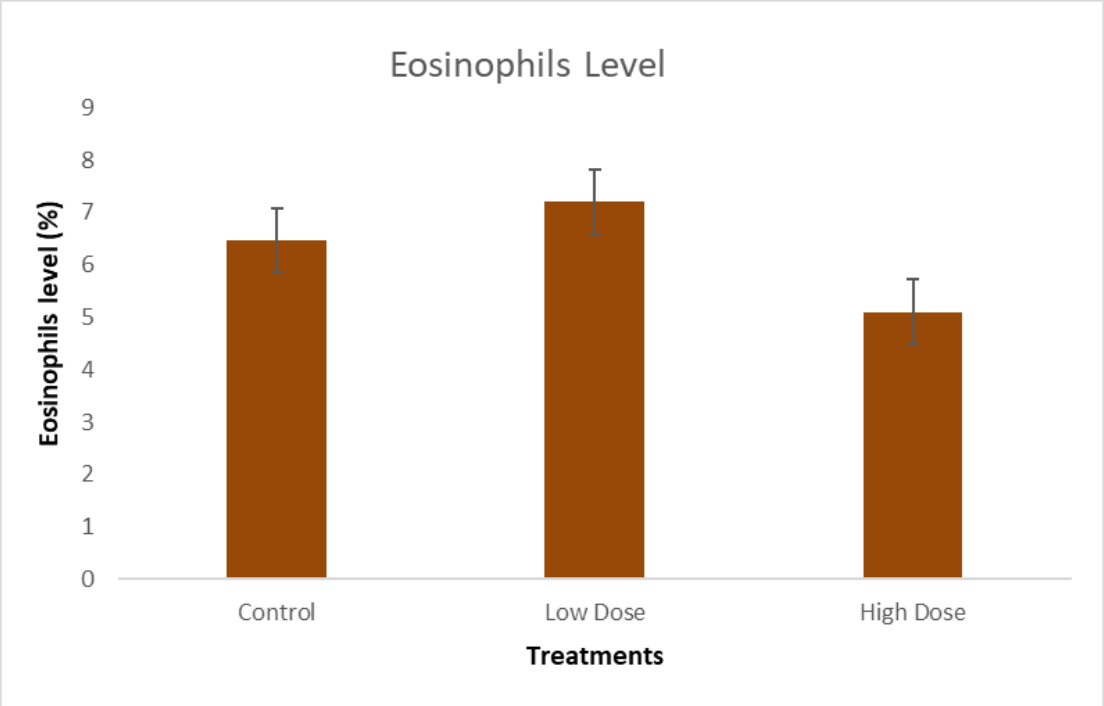

FIGURE 4.17: Graphical presentation of Eosinophils level (%) of all groups

TABLE 4.10: Mean±SD values of Eosinophils count for all groups compared by one way ANOVA

Parameter	Control	Low Dose	High Dose	P value
Eosinophils	6.46±0.55	7.2± 0.2	5.1±0.1	0.0008

4.5.9 MCHC

Mean Corpuscular Hemoglobin Concentration (MCHC) reflects the average concentration of hemoglobin in red blood cells and is used to assess types of anemia or red cell disorders. Changes in MCHC can indicate alterations in hemoglobin synthesis or red blood cell integrity [72].

According to the table, MCHC levels vary significantly across groups (P = 0.04). The low dose group shows a slight decrease (33.23 ± 1.07) compared to control (35.26 ± 0.83), while the high dose group exhibits a mild increase (36.13 ± 1.10). This suggests that the treatment influences hemoglobin concentration in a dose-dependent manner, with higher doses potentially enhancing hemoglobin content within red blood cells.

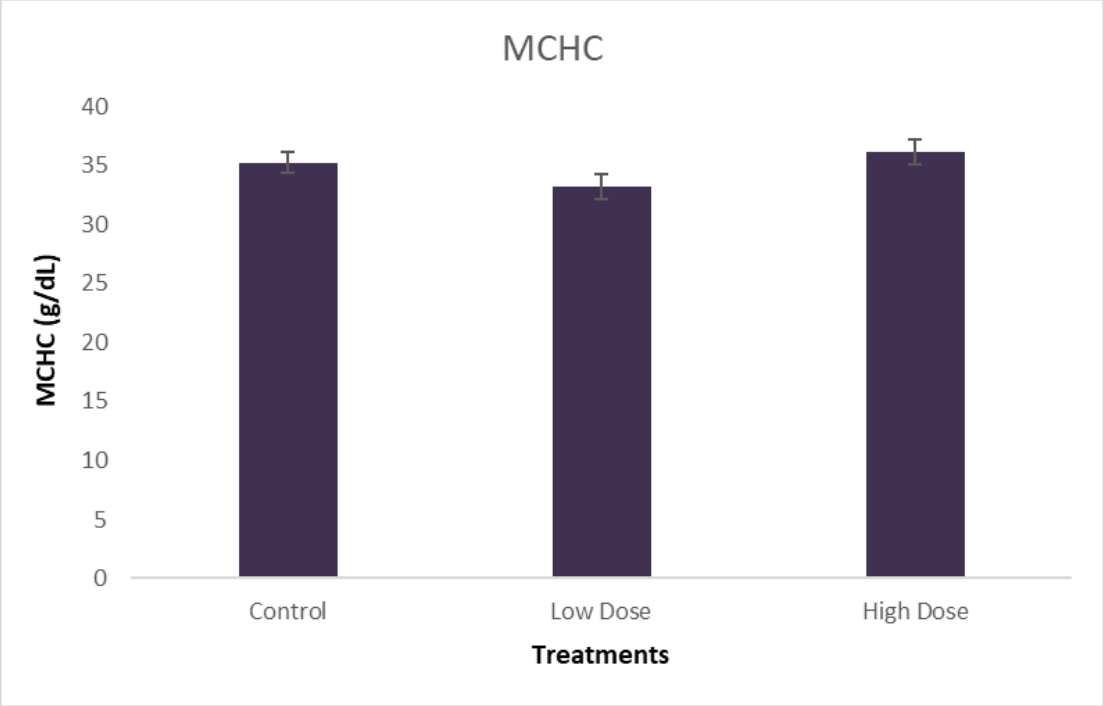

FIGURE 4.18: Graphical presentation of Eosinophils level (%) of all groups

TABLE 4.11: Mean±SD values of MCHC count for all groups compared by one way ANOVA

Parameter	**Control**	**Low Dose**	**High Dose**	**P value**
MCHC	35.26±0.83	33.23±1.069	36.13+1.096	0.04

4.5.10 HCT

Hematocrit (HCT) measures the proportion of red blood cells in the blood and is an important indicator of oxygen-carrying capacity and overall blood health. Changes in HCT can reflect dehydration, anemia, or other blood disorders [73].

In this table, HCT levels show a slight decrease from control (39.33 ± 4.24) to low dose (35.13 ± 0.15) and high dose (34 ± 0.3), but the difference is not statistically significant (P = 0.08).

This suggests that the treatment may have a mild lowering effect on red blood cell volume, though the evidence is not strong enough to confirm a definitive impact.

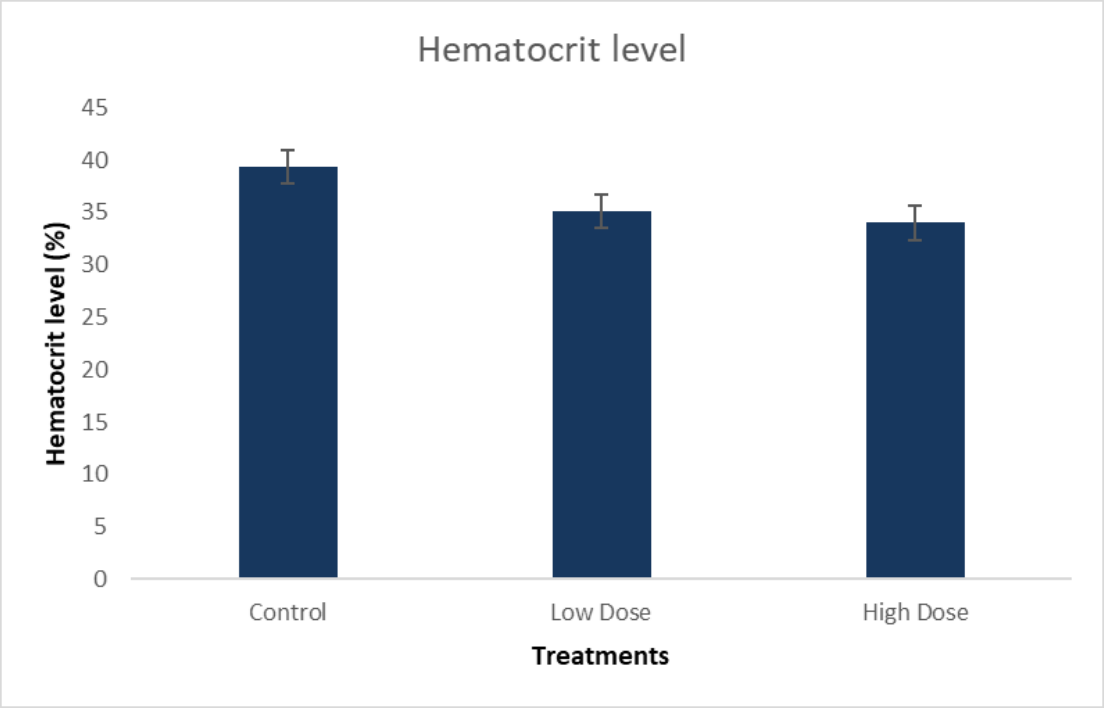

FIGURE 4.19: Graphical presentation of HCT levels%

TABLE 4.12: Mean±SD values of HCT count for all groups compared by one way ANOVA

Parameter	Control	Low Dose	High Dose	P value
HCT	39.33±4.24	35.13±0.152	34± 0.3	0.08

4.5.11 MCV

Mean Corpuscular Volume (MCV) measures the average size of red blood cells and helps diagnose different types of anemia. Increased MCV values typically indicate larger-than-normal red blood cells, which can be associated with conditions like vitamin B12 deficiency or bone marrow response [74].

The table shows a significant increase in MCV levels in both low dose (54.1 ± 0.75) and high dose (55.5 ± 0.1) groups compared to control (45.03 ± 1.20), with a P value of 0.008.

This suggests that the treatment causes red blood cells to become larger, indicating a possible effect on red blood cell production or maturation.

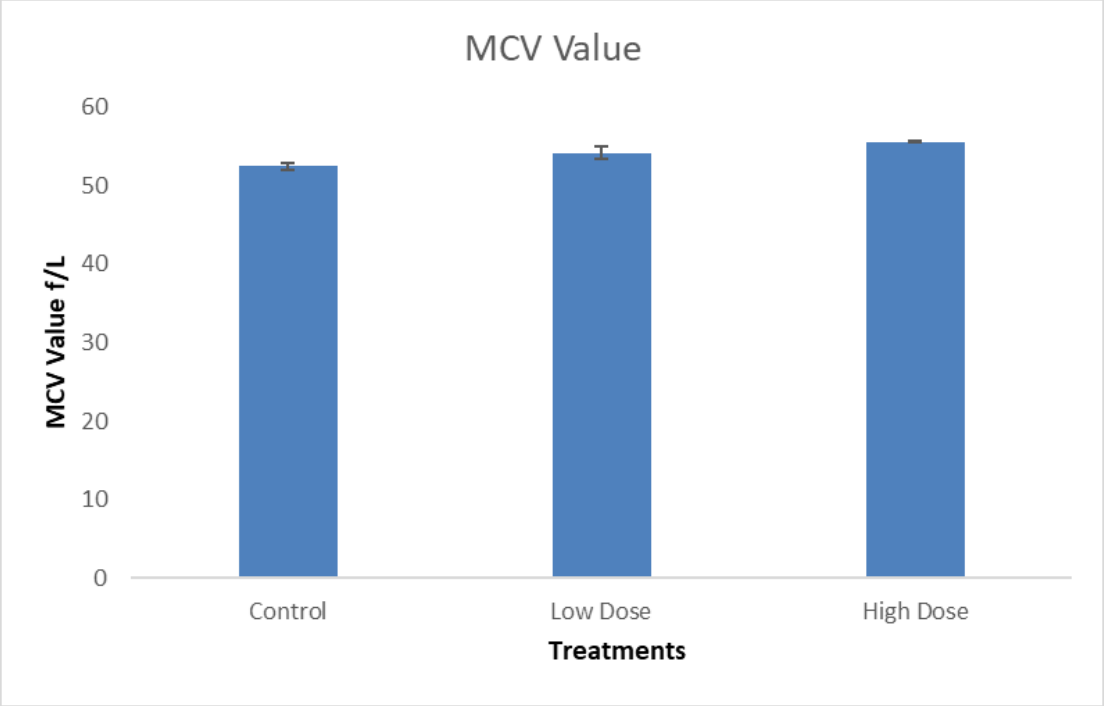

FIGURE 4.20: MCV levels (f/l) graphical presentation

TABLE 4.13: Mean±SD values of MCV levels for all groups compared by one way ANOVA

Parameter	Control	Low Dose	High Dose	P value
MCV	45.03±1.20	54.1±0.754	55.5+0.1	0.008

4.5.12 MCH

Mean Corpuscular Hemoglobin (MCH) measures the average amount of hemoglobin per red blood cell and is important for assessing red blood cell function and oxygen-carrying capacity [75].

The table shows a significant increase in MCH levels in both the low dose (19 ± 0.2) and high dose (19.8 ± 0.36) groups compared to the control (15.6 ± 0.70), with a highly significant P value of 0.0001.

This indicates that the treatment substantially raises the hemoglobin content in individual red blood cells, which may improve their oxygen transport efficiency.

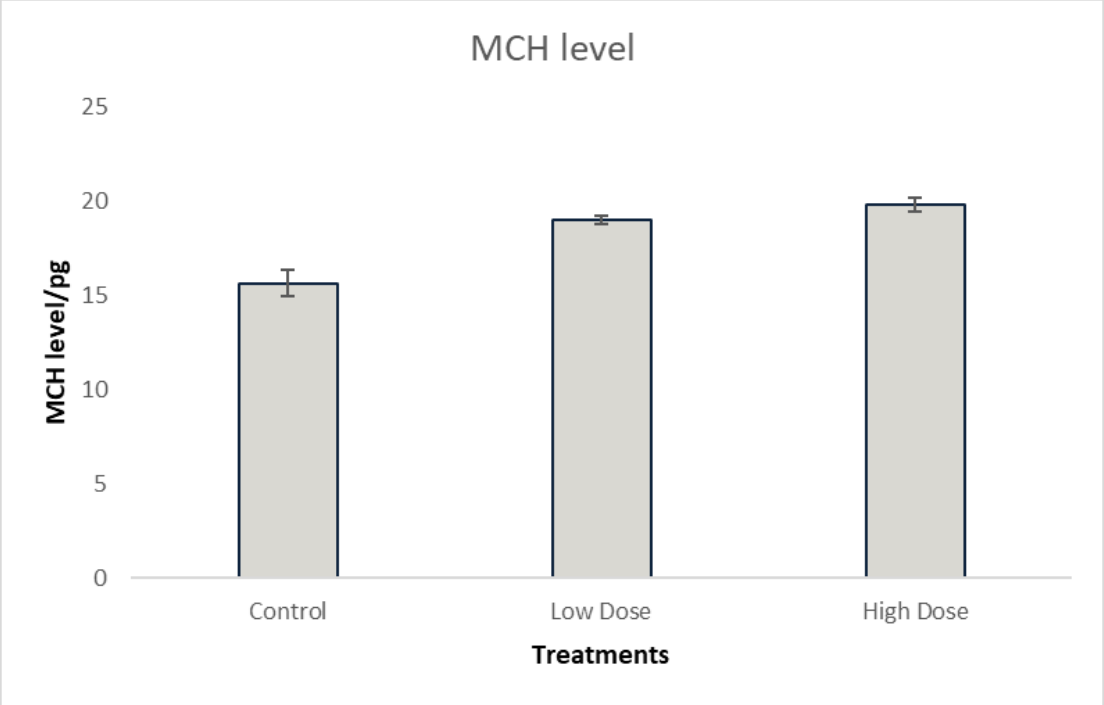

FIGURE 4.21: MCH (p g) level of all groups, when p value was <0.05

TABLE 4.14: MCH levels of control, low dose and high dose group compared in one way ANOVA

Parameter	Control	Low Dose	High Dose	P value
MCH	15.6±0.70	19±0.2	19.8+0.36	0.0001

4.6 Renal Functioning Tests

4.6.1 Creatinine

Creatinine is a waste product produced by muscle metabolism and is commonly measured to assess kidney function. Stable creatinine levels generally indicate normal kidney health [76].

In this table, creatinine levels remain similar across control (0.92 ± 0.16), low dose (0.99 ± 0.05), and high dose (0.95 ± 0.14) groups, with a non-significant P value of 0.78. This suggests that the treatment does not have a significant effect on kidney function based on creatinine measurements.

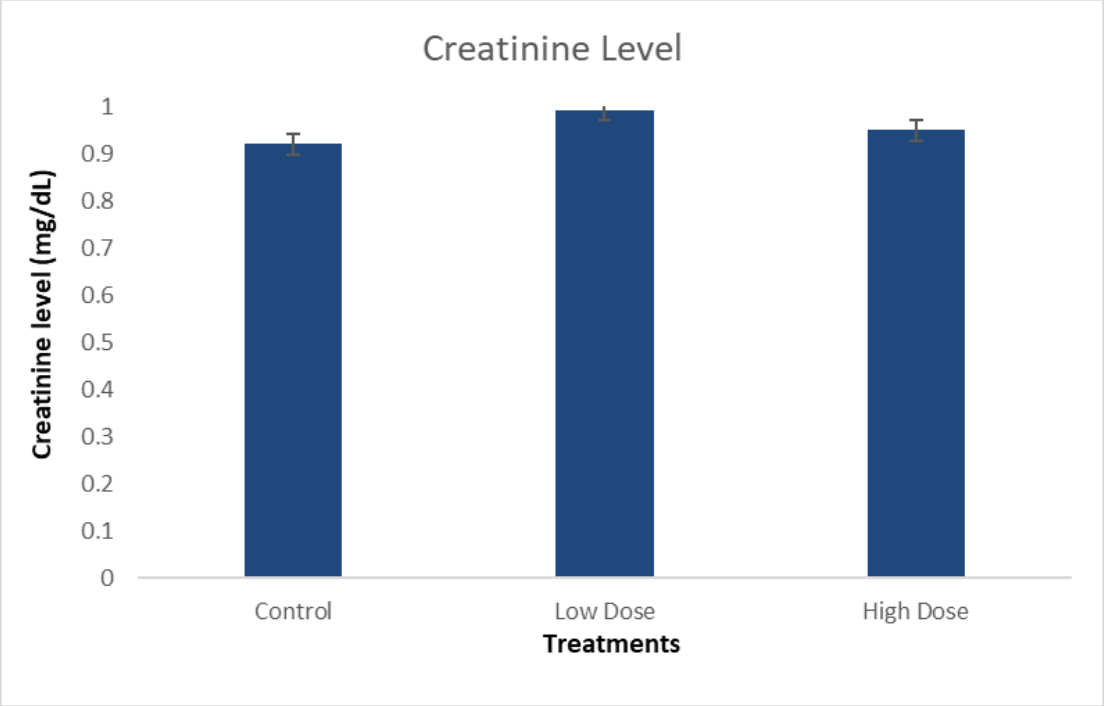

FIGURE 4.22: Creatinine (mg/dL) value of all groups.

TABLE 4.15: Mean±SD values for Creatinine of all groups compared by one way ANOVA

Parameter	**Control**	**Low Dose**	**High Dose**	**P value**
Creatinine	0.92± 0.16	0.99± 0.05	0.95± 0.14	0.78

4.6.2 BUN

Blood Urea Nitrogen (BUN) is a marker of kidney function and protein metabolism, reflecting how well the kidneys are removing waste from the blood [77].

The table shows a significant difference in BUN levels across groups (P = 0.008). The low dose group has a slight increase (14.4 ± 0.8) compared to control (13.63 ± 0.25), while the high dose group shows a decrease (12.4 ± 0.3).

This suggests that the treatment affects kidney function or protein metabolism in a dose-dependent manner, with higher doses potentially improving or normalizing BUN levels.

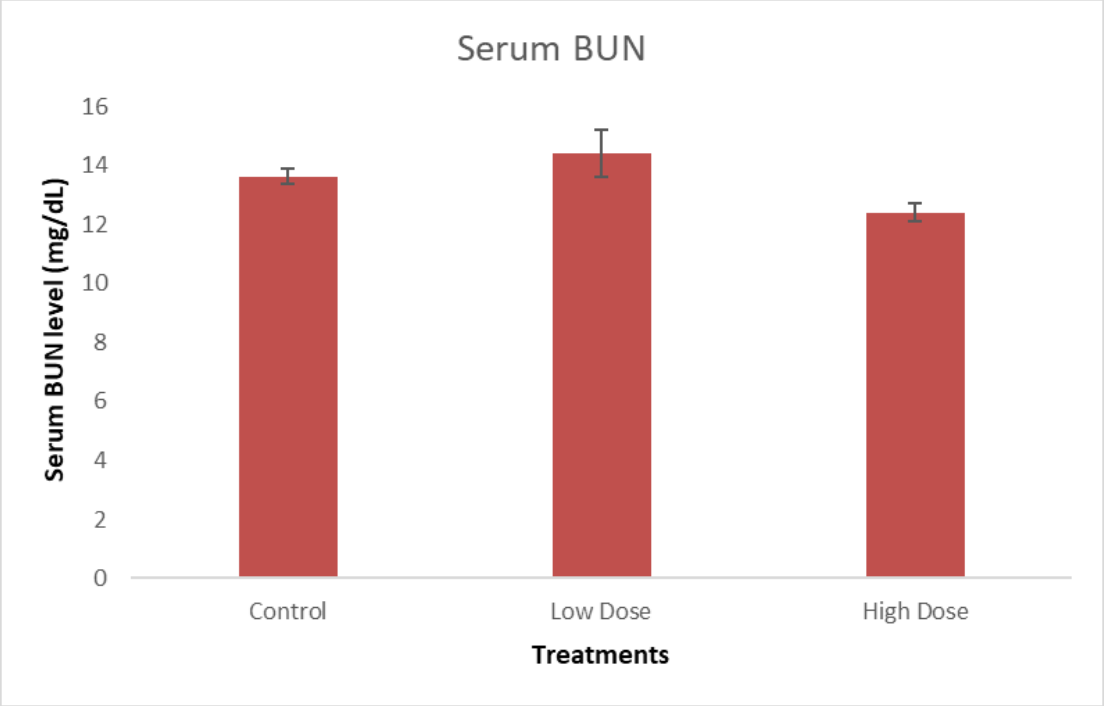

FIGURE 4.23: BUN (mg/dL) value of all groups

TABLE 4.16: Mean±SD values for BUN of all groups compared by one-way ANOVA

Parameter	**Control**	**Low Dose**	**High Dose**	**P value**
BUN	13.63± 0.25	14.4± 0.8	12.4± 0.3	0.008

4.6.3 Urea

Urea is a waste product formed from protein metabolism and is commonly measured to assess kidney function and nitrogen balance.

In this table, urea levels show a slight increase in the low dose group (30.5 ± 2.12) and a decrease in the high dose group (26.5 ± 0.70) compared to control (29.5 ± 0.70).

However, the differences are not statistically significant (P = 0.11), indicating that the treatment does not have a clear impact on urea levels or kidney function in this context.

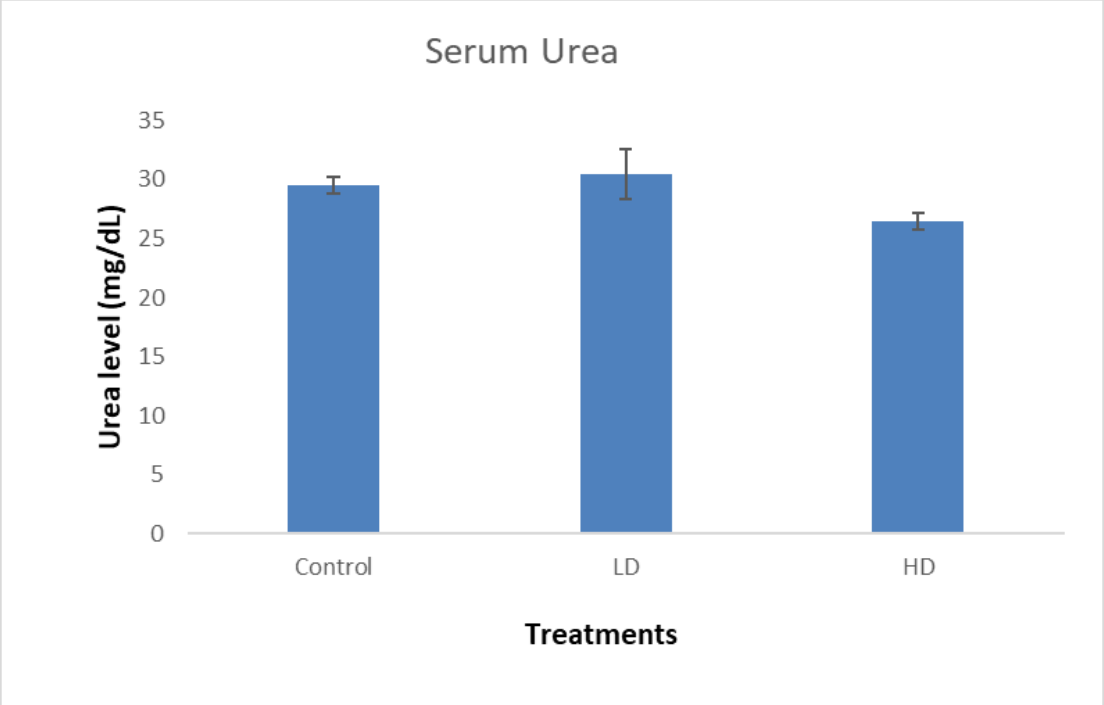

FIGURE 4.24: Urea (mg/dL) value of all groups

TABLE 4.17: Mean±SD values for Urea of all groups compared by one-way ANOVA

Parameter	Control	Low Dose	High Dose	P value
Urea	29.5 ± 0.70	30.5 ± 2.12	26.5 ± 0.70	0.11

4.7 Liver Function Test (LFT)

4.7.1 ALT

Alanine aminotransferase (ALT) is an enzyme found mainly in the liver, and elevated levels in the blood typically indicate liver injury or inflammation [79].

The table shows a significant increase in ALT levels across groups ($P = 0.028$), with the low dose group at 67.3 ± 5.5 and the high dose group at 95 ± 20, compared to the control group at 53 ± 13. This suggests that the treatment may cause liver stress or damage in a dose-dependent manner, with higher doses leading to greater liver enzyme elevation.

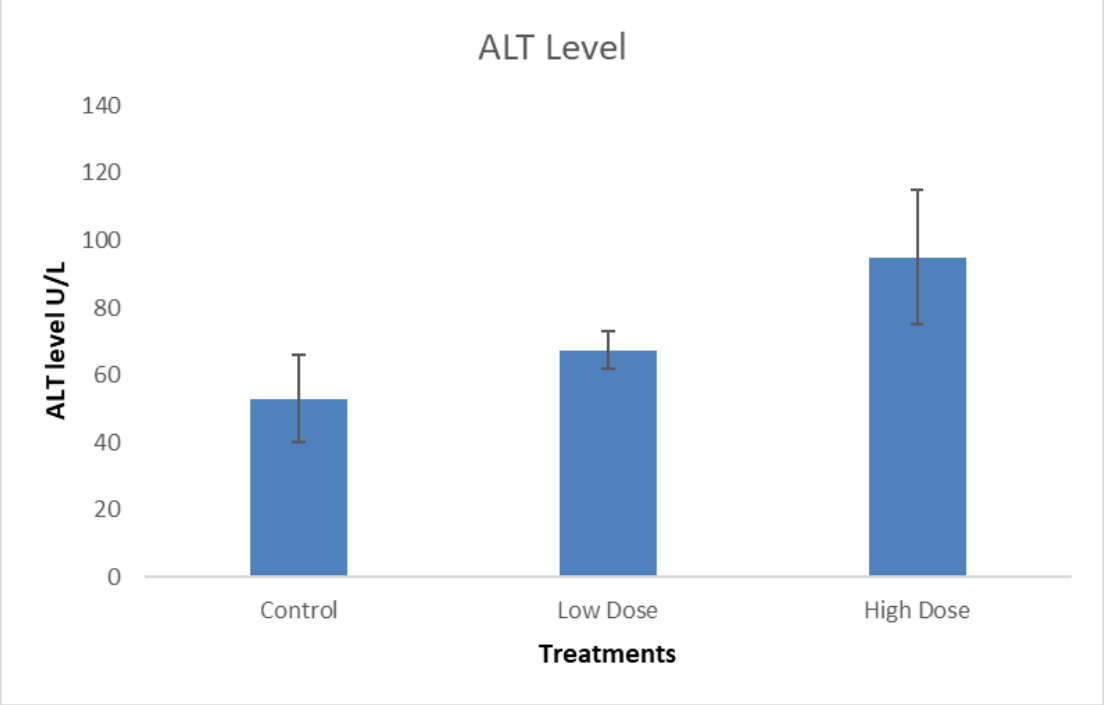

FIGURE 4.25: Graphical presentation of ALT (U/L) value of all groups

TABLE 4.18: Mean±SD values for ALT of all groups compared by one-way

Parameter	Control	Low Dose	High Dose	P value
ALT	53± 13	67.3± 5.50	95+ 20	0.028

4.7.2 Albumin

Albumin is a major blood protein produced by the liver, important for maintaining blood volume and transporting substances [80].

In the table, albumin levels show a slight decrease in the low dose group (3.56 ± 0.06) compared to control (3.69 ± 0.09), while the high dose group shows a notable increase (5.42 ± 1.47).

However, the difference is not statistically significant (P = 0.06), suggesting a possible trend toward increased albumin at higher doses but without strong evidence to confirm this effect

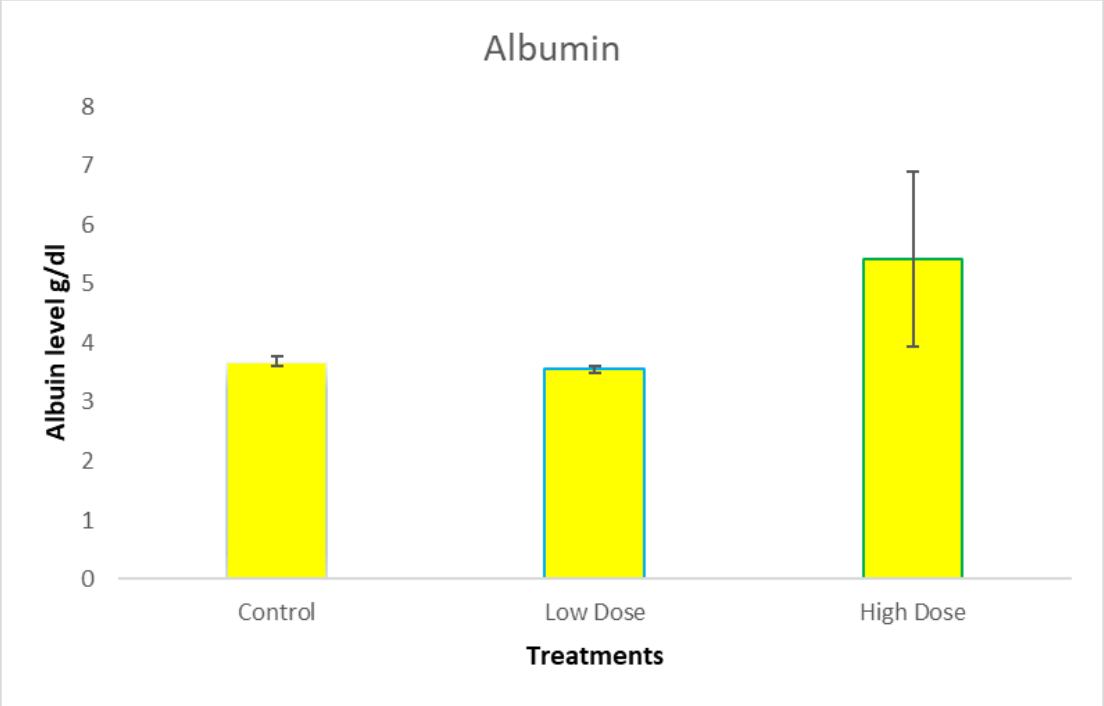

FIGURE 4.26: Albumin (g/dL) value of all groups

TABLE 4.19: Mean±SD values for Albumin of all groups compared by one way ANOVA

Parameter	Control	Low Dose	High Dose	P value
Albumin	3.69± 0.09	3.56± 0.06	5.42+ 1.47	0.06

4.7.3 Total Protein

Total protein measures the combined amount of all proteins in the blood, including albumin and globulins, and reflects overall nutritional and liver status [81]. In the table, total protein levels are fairly consistent across control (7.56 ± 0.36), low dose (7.66 ± 0.38), and high dose (7.05 ± 0.16) groups, with no significant difference (P = 0.112).

In the table, total protein levels are fairly consistent across control (7.56 ± 0.36), low dose (7.66 ± 0.38), and high dose (7.05 ± 0.16) groups, with no significant difference (P = 0.112). This indicates that the treatment does not significantly affect total protein levels.

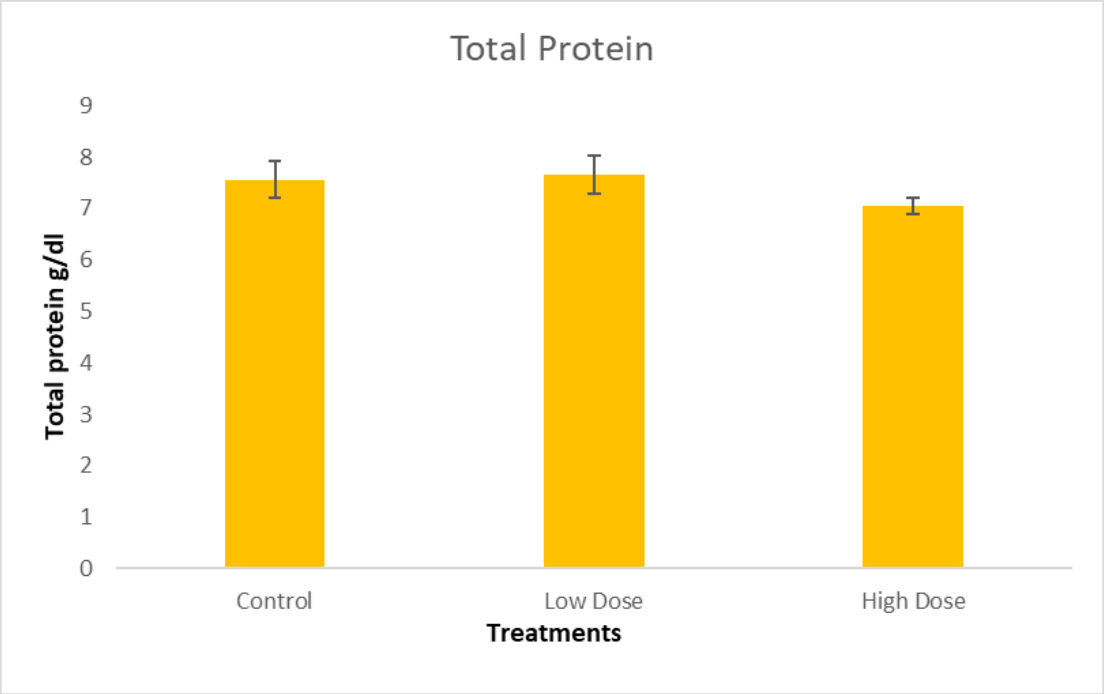

FIGURE 4.27: Graphical presentation of Total protein g/dl of all groups

TABLE 4.20: Comparison of Control, Low and High dose group in one way ANOVA

Parameter	Control	Low Dose	High Dose	P value
Total Protein	7.56± 0.36	7.66± 0.38	7.05+ 0.16	0.112

4.7.4 Bilirubin

Bilirubin is a breakdown product of red blood cells and is commonly measured to assess liver function and bile flow [82]. In the table, bilirubin levels remain stable between the control and low dose groups (0.1), with a slight increase in the high dose group (0.2 ± 0.1).

In the table, bilirubin levels remain stable between the control and low dose groups (0.1), with a slight increase in the high dose group (0.2 ± 0.1).

However, this change is not statistically significant (P = 0.12), suggesting the treatment does not have a clear impact on bilirubin levels or liver function in this study.

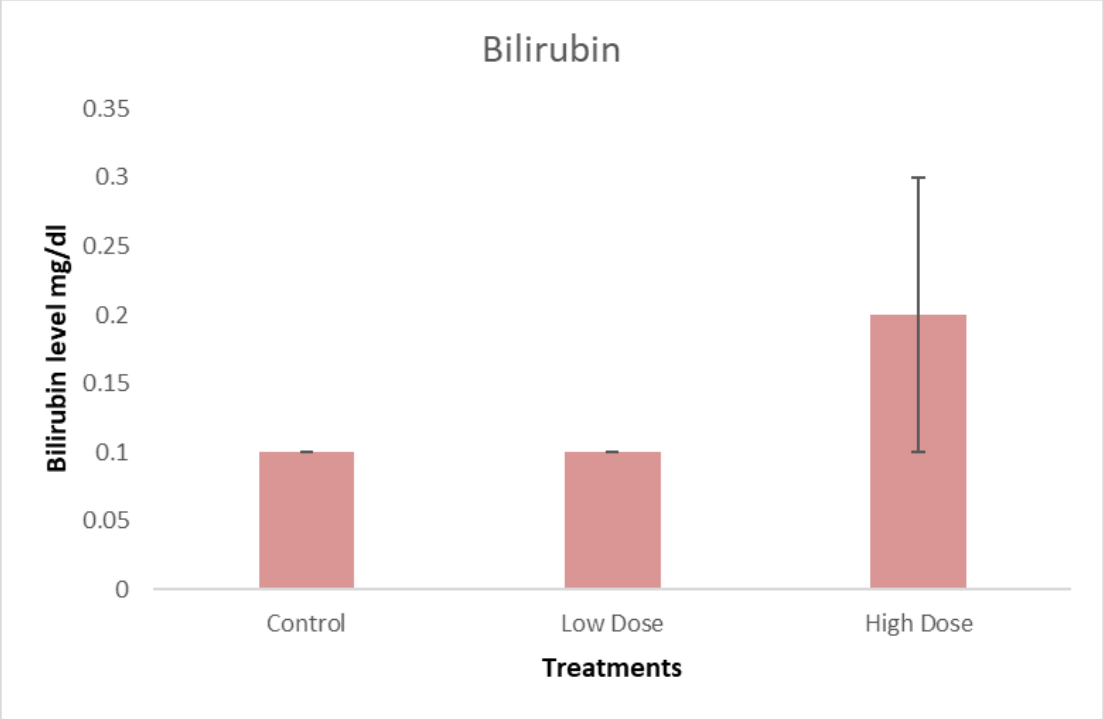

FIGURE 4.28: Bilirubin Total (U/L) value of all groups

TABLE 4.21: Mean±SD values for Bilirubin of all groups compared by one way ANOVA

Parameter	Control	Low Dose	High Dose	P value
Bilirubin	0.1	0.1	0.2+ 0.1	0.12

4.7.5 Globulins

Globulins are a group of blood proteins involved in immune responses, including antibodies [83]. The table shows a slight increase in globulin levels in the low dose group (4.1 ± 0.44) compared to control (3.88 ± 0.27), and a decrease in the high dose group (3.4 ± 0.13). However, these changes are not statistically significant (P = 0.07), indicating only a trend toward modulation of immune-related proteins without strong evidence of a treatment effect.

However, these changes are not statistically significant (P = 0.07), indicating only a trend toward modulation of immune-related proteins without strong evidence of a treatment effect.

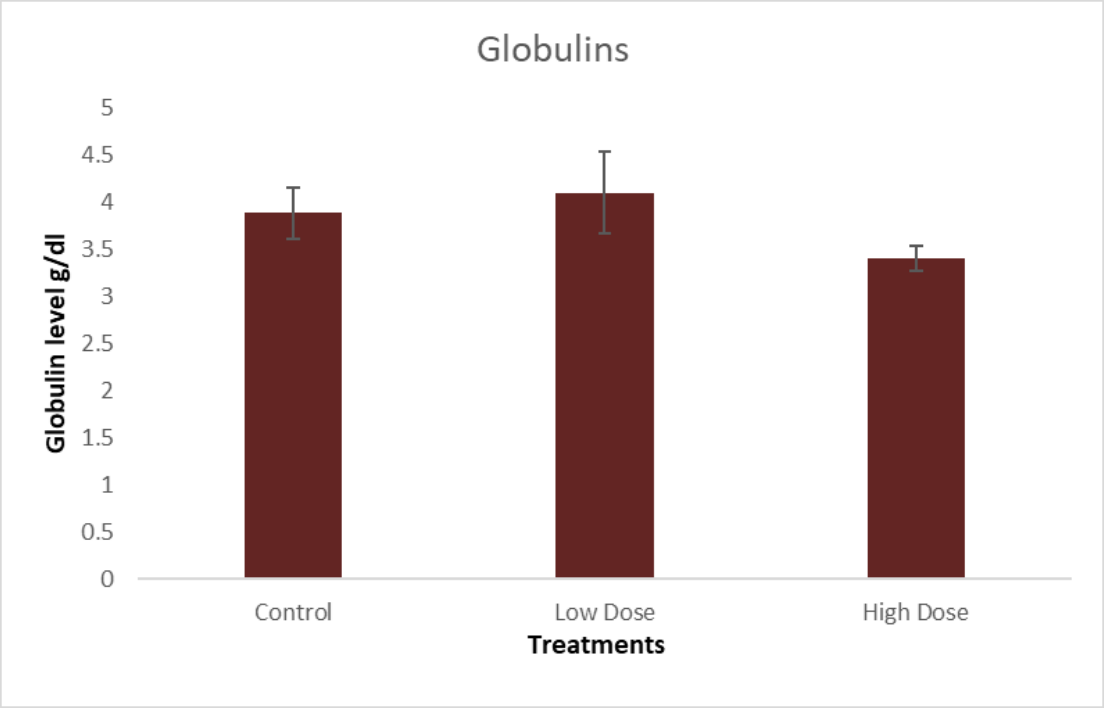

FIGURE 4.29: Globulin level g/dl of all groups

TABLE 4.22: Mean±SD values for Globulins of all groups compared by one way ANOVA

Parameter	Control	Low Dose	High Dose	P value
Globulins	3.88± 0.27	4.1±0.44	3.4+ 0.13	0.07

4.8 Histopathology of Liver

4.8.1 Control group

The liver histopathology section exhibits a relatively preserved hepatic architecture with mild pathological changes. The hepatocytes are arranged in a typical lobular pattern, radiating from the central vein. However, there is evidence of mild hepatocellular vacuolation. Mild sinusoidal congestion is visible, indicating minor circulatory disturbances. No significant necrosis or fibrosis is observed in this section. Mild sinusoidal congestion is visible, indicating minor circulatory disturbances. No significant necrosis or fibrosis is observed in this section.

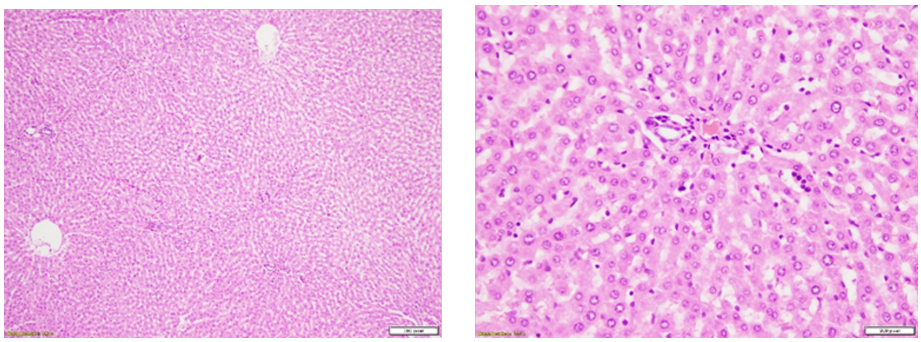

FIGURE 4.30: Histopathological analysis of liver tissues at 10 and 40x, Control group

4.8.2 Low Dose Group

The histopathological section of liver tissue exhibits a well-defined, dense aggregate of inflammatory cells (star), predominantly lymphocytes and macrophages, indicative of a focal granulomatous. The surrounding hepatocytes appear largely intact but display mild vacuolar degeneration. The inflammatory infiltrate is centered around a portal region, suggesting a portal-based inflammatory response. The presence of lymphocytic infiltration and hepatocyte degeneration suggests ongoing hepatic injury.

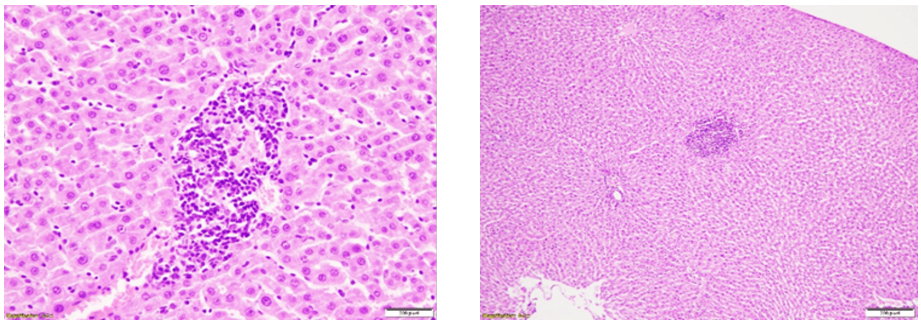

FIGURE 4.31: Histopathological analysis of liver tissues of low dose group

4.8.3 High Dose Group

The histopathological section of the liver shows evidence of hepatocellular degeneration and mild inflammation. Hepatocytes display cytoplasmic vacuolation, indicating possible hydropic or fatty degeneration. There are scattered foci of

inflammatory cell infiltration, primarily composed of mononuclear cells (arrow), suggesting a mild inflammatory response. The presence of sinusoidal congestion and hemorrhagic areas (arrow head) indicates vascular disturbances. Some hepatocytes exhibit pyknotic nuclei (red arrow), which may indicate early apoptosis or necrosis.

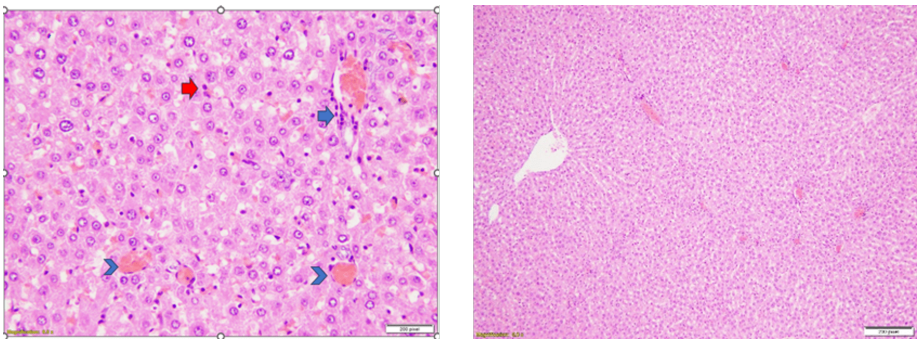

FIGURE 4.32: Histopathological analysis of liver tissues, high dose group

Chapter 5

Discussion

The present study investigated the in-vivo toxicity and biological safety of magnesium sulfide nanoparticles (MgS-NPs) synthesized through a green method using Citrus limetta leaf extract. This research provides a comprehensive insight into the growing field of green nanotechnology and its implications for biomedical applications. The novelty of this study lies not only in the synthesis approach but also in its holistic biological evaluation, combining hematological, biochemical, and histopathological analysis.

The results of the study revealed a clear dose-dependent biological response. High-dose MgS-NPs (3.46 mg/200g) significantly altered serum biomarkers such as ALT, AST, urea, and creatinine, which are well-established indicators of liver and kidney function. These biochemical disruptions were supported by histological evidence of hepatocellular degeneration, vacuolization, inflammation, and pyknotic nuclei, indicating cellular distress and the initiation of apoptosis. These outcomes are consistent with pr...

In contrast, the low-dose group (1.73 mg/200g) showed only mild histological alterations and minimal changes in biochemical markers, suggesting that at lower concentrations, green-synthesized MgS-NPs may be better tolerated by biological systems. This aligns with the work of Ali *et al.* (2023)[84], who demonstrated that MgO NPs synthesized using Abrus precatorius bark extract were effective and exhibited low cytotoxicity at reduced concentrations.

Notably, the antioxidant and antimicrobial properties of Citrus limetta, as reported by Mahmood *et al.* (2022)[85], may have contributed to the relatively safer profile of the low-dose MgS-NPs. Citrus limetta leaves contain flavonoids, alkaloids, and phenolics, which could stabilize the nanoparticles and mitigate oxidative stress. The use of plant extracts in nanoparticle synthesis is known to introduce capping agents that influence biological interactions (Gupta *et al.*, 2023; Hano & Abbasi, 2021)[86].

However, despite their green origin, nanoparticles can exhibit toxicity depending on their size, surface chemistry, and concentration (Sajid & Płotka-Wasylka, 2020)[87]. Our findings support this by highlighting the adverse effects of high-dose MgS-NPs, reinforcing the concept that green synthesis alone does not ensure biosafety.

The results also align with Bukola *et al.* (2018)[88], who observed significant liver and kidney damage in rats exposed to magnesium hydroxide nanoparticles for 28 days.

Comparing MgS-NPs with other metal sulfide nanoparticles further contextualizes their safety. Rana *et al.* (2018)[89] reported severe nephrotoxicity with cadmium sulfide (CdS) NPs even at low doses, while lead sulfide NPs are known for inducing oxidative stress and pulmonary inflammation (Ghasempour *et al.*, 2023)[90]. In this regard, MgS-NPs appear to be relatively less toxic, possibly due to the essential biological roles of magnesium and sulfur (Ahmed *et al.*, 2023)[91]. Magnesium is a cofactor in numerous enzymatic reactions, and sulfur contributes to amino acids and antioxidants like glutathione.

The in vitro findings of Nalci *et al.* (2020)[92], who investigated MgS-Cisplatin nanoconjugates on neuroblastoma cells, showed promising anticancer effects without significant cytotoxicity. However, our in vivo data reveal that systemic administration, especially at higher concentrations, introduces a risk of tissue toxicity, which may not be evident in isolated cellular environments. This highlights the importance of animal studies in bridging the gap between laboratory results and clinical relevance.

Furthermore, studies on the biodistribution and pharmacokinetics of nanoparticles emphasize that surface functionalization, particle charge, and aggregation state play crucial roles in toxicity (Altammar, 2023; Rizvi & Saleh, 2018)[93]. Nanoparticles may accumulate in specific organs like the liver, spleen, and kidneys, leading to oxidative stress, inflammation, and cellular damage over time.

The results also support previous studies on the biocompatibility of Mg-based NPs. For instance, Ali *et al.* (2023)[94] found MgO NPs to be safe at low doses, while Gatou *et al.* (2024)[95] emphasized that MgO NPs are best suited for therapeutic use when appropriately dosed. Similarly, green-synthesized ZnO and CuO NPs have demonstrated antimicrobial and anticancer potential with varying toxicity profiles depending on synthesis route and dose (Islam *et al.*, 2022; Sudhakar *et al.*, 2025)[96].

Histopathological findings in this study, such as vacuolar degeneration and early signs of apoptosis, mirror those reported by Alwan *et al.* (2021)[97] in rats exposed to biogenic AgNPs, and by Khan *et al.* (2025)[98] in ZnS and ZnO nanocomposites. These morphological changes reinforce that even low-toxicity nanoparticles can elicit tissue-level stress responses if not optimally administered.

Taken together, the findings of this study support the growing consensus that green-synthesized nanoparticles, while environmentally sustainable and potentially safer, must undergo thorough in-vivo testing to establish realistic dose thresholds and understand long-term biological impacts. The moderate toxicity observed at high doses of MgS-NPs underscores the importance of careful risk-benefit analysis before biomedical applications.

Chapter 6

Conclusion and Future Work

This study explored the in-vivo toxicity and biological safety of magnesium sulfide nanoparticles (MgS-NPs) synthesized through a green method using Citrus limetta leaf extract. Through a 20-day experimental trial on Sprague Dawley rats, the research provided a thorough evaluation of how these nanoparticles interact with living systems. The use of Citrus limetta leaves not only offered a sustainable and eco-friendly synthesis route but also introduced bioactive compounds that likely contributed to the stabilization and modulation of the nanoparticle activity.

The findings demonstrated a clear dose-dependent effect. At higher concentrations (3.46 mg/200g), MgS-NPs triggered notable biological responses, including elevated liver enzymes, disrupted kidney markers, and distinct histological alterations such as hepatocellular degeneration and pyknotic nuclei suggesting early cell death. These changes reflect the stress nanoparticles can impose on the liver and kidneys when present in higher quantities. On the other hand, the group receiving a lower dose (1.73 mg/200g) showed only mild deviations from the control, indicating that such concentrations might be within a safer threshold for future biomedical use.

It is encouraging to note that the elemental composition of MgS built from magnesium and sulfur, both of which are naturally present in the body may help explain why these nanoparticles are less toxic compared to other metal sulfides like cadmium or lead-based compounds. However, the mere fact that these nanoparticles

are synthesized through a green route or made of biocompatible elements does not guarantee their absolute safety. This study highlights the importance of rigorous in-vivo assessments in addition to in-vitro analyses to accurately understand their biological impact.

Overall, this research lays a strong foundation for future exploration into magnesium-based nanomaterials. The results support the potential of MgS-NPs for biomedical applications but clearly emphasize the need for careful dosage regulation and long-term toxicity studies. By identifying both safe and harmful thresholds, this work contributes valuable insights to the responsible development of nanotechnology in medicine.

While this study has contributed significantly to the understanding of MgS nanoparticle safety, it also opens several doors for future investigations.

1. Firstly, the 20-day experimental period provided important initial insights, but it remains unclear how chronic exposure to MgS-NPs might affect living systems. Long-term toxicity studies, possibly spanning several months, are necessary to assess bioaccumulation and delayed onset of organ dysfunction.

2. Secondly, this study did not delve into the molecular mechanisms behind the observed toxic effects. Future research should explore oxidative stress pathways, mitochondrial damage, and inflammatory signaling to provide a mechanistic understanding of nanoparticle behavior inside the body.

3. Techniques such as gene expression analysis and proteomics could greatly enhance this aspect. Moreover, identifying the ideal dosage for therapeutic use requires testing a broader range of nanoparticle concentrations. Establishing a precise therapeutic index the balance between efficacy and safety will be crucial before any clinical application.

4. Tracking how these nanoparticles distribute across organs, and how they are metabolized and excreted, is another vital area. Advanced tools such as radio-labeling or ICP-MS can provide real-time biodistribution and pharmacokinetic data, helping to assess potential off-target effects.

5. In addition, comparative studies using other plant-based synthesis methods could highlight whether Citrus limetta holds unique advantages, or if similar effects are found with different botanical sources. Comparing MgS-NPs with other metallic or non-metallic nanoparticles would further broaden our understanding.

6. Lastly, while rats provide a strong baseline for toxicological testing, validation in other animal models and human cell lines will bring the findings closer to clinical relevance. Applications in drug delivery, cancer therapy, or antimicrobial treatments should be pursued, but only after thorough evaluations ensure safety and efficacy.

In conclusion, this study is a starting point. It confirms that green-synthesized MgS-NPs are not inherently safe or toxic they are dose-dependent. As research moves forward, deeper investigations into mechanisms, pharmacology, and real-world applications will be key to unlocking their full potential in the biomedical field.

Bibliography

[1] D. Astruc, "Introduction: Nanoparticles in Catalysis," Chem. Rev., vol. 120, no. 2, pp. 461–463, Jan. 2020.

[2] Z. Morshedtalab et al., "Antibacterial Assessment of Zinc Sulfide Nanoparticles against Streptococcus pyogenes and Acinetobacter baumannii," Curr. Top. Med. Chem., vol. 20, no. 11, pp. 1042–1055, 2020.

[3] N. Joudeh and D. Linke, "Nanoparticle classification, physicochemical properties, characterization, and applications: a comprehensive review for biologists," J. Nanobiotechnol., vol. 20, no. 1, p. 262, 2022.

[4] N. Hossain et al., "Advances and significances of nanoparticles in semiconductor applications – A review," Results Eng., vol. 19, p. 101347, 2023.

[5] D. Latha, S. Sampurnam, C. Arulvasu, P. Prabu, K. Govindaraju, and V. Narayanan, "Biosynthesis and characterization of gold nanoparticle from Justicia adhatoda and its catalytic activity," Mater. Today Proc., vol. 5, no. 2, pp. 8968–8972, 2018.

[6] C. Sudhakar et al., "Eco-friendly green synthesis and characterization of zirconium oxide nanoparticles using Ulva lactuca and their medical and environmental potential," J. Environ. Chem. Eng., vol. 13, no. 2, p. 115862, 2025.

[7] S. Naz, S. T. B. Kazmi, and M. Zia, "CeO_2 nanoparticles synthesized through green chemistry are biocompatible: In vitro and in vivo assessment," J. Biochem. Mol. Toxicol., vol. 33, no. 5, p. e22291, 2019.

[8] D. Gupta, A. Boora, A. Thakur, and T. K. Gupta, "Green and sustainable synthesis of nanomaterials: Recent advancements and limitations," Environ. Res., vol. 231, p. 116316, 2023.

[9] J. Annamalai, S. B. Ummalyma, A. Pandey, and T. Bhaskar, "Recent trends in microbial nanoparticle synthesis and potential application in environmental technology: a comprehensive review," Environ. Sci. Pollut. Res. Int., vol. 28, no. 36, pp. 49362–49382, 2021.

[10] M. Sajid and J. Płotka-Wasylka, "Nanoparticles: Synthesis, characteristics, and applications in analytical and other sciences," Microchem. J., vol. 154, p. 104623, 2020.

[11] S. Ali et al., "Green Synthesis of Magnesium Oxide Nanoparticles by Using Abrus precatorius Bark Extract and Their Photocatalytic, Antioxidant, Antibacterial, and Cytotoxicity Activities," Bioengineering, vol. 10, no. 3, p. 302, 2023.

[12] R. B. Rotti et al., "Green synthesis of MgO nanoparticles and its antibacterial properties," Front. Chem., vol. 11, p. 1143614, 2023.

[13] M.-A. Gatou et al., "Magnesium Oxide (MgO) Nanoparticles: Synthetic Strategies and Biomedical Applications," Crystals, vol. 14, no. 3, p. 215, 2024.

[14] A. Bukola, O. Oloyede, O. Adewale, O. Olalekan, Y. A. S. Ajimoko, and M. Ogundare, "Toxicological evaluation of magnesium hydroxide nanoparticles in rats following 28 days of repeated oral exposure," Pharmacologyonline, vol. 2, pp. 263–273, 2018.

[15] A. Ghasempour et al., "Cadmium Sulfide Nanoparticles: Preparation, Characterization, and Biomedical Applications," Molecules, vol. 28, no. 9, 2023.

[16] K. Rana, Y. Verma, V. Rani, and S. V. S. Rana, "Renal toxicity of nanoparticles of cadmium sulphide in rat," Chemosphere, vol. 193, pp. 142–150, 2018.

[17] O. B. Nalci, H. Nadaroglu, S. Genc, A. Hacimuftuoglu, and A. Alayli, "The effects of MgS nanoparticles-Cisplatin-bio-conjugate on SH-SY5Y neuroblastoma cell line," Mol. Biol. Rep., vol. 47, no. 12, pp. 9715–9723, 2020.

[18] N. Ahmed et al., "The power of magnesium: unlocking the potential for increased yield, quality, and stress tolerance of horticultural crops," Front. Plant Sci., vol. 14, p. 1285512, 2023.

[19] Q. Zhao, N. Cheng, X. Sun, L. Yan, and W. Li, "The application of nanomedicine in clinical settings," Front. Bioeng. Biotechnol., vol. 11, p. 1219054, 2023.

[20] B. Han, W. H. Fang, S. Zhao, Z. Yang, and B. X. Hoang, "Zinc sulfide nanoparticles improve skin regeneration," Nanomedicine, vol. 29, p. 102263, 2020.

[21] N. Zahin et al., "Nanoparticles and its biomedical applications in health and diseases: special focus on drug delivery," Environ. Sci. Pollut. Res., vol. 27, no. 16, pp. 19151–19168, 2020.

[22] K. A. Altammar, "A review on nanoparticles: characteristics, synthesis, applications, and challenges," Front. Microbiol., vol. 14, p. 1155622, 2023.

[23] A. A. Yetisgin, S. Cetinel, M. Zuvin, A. Kosar, and O. Kutlu, "Therapeutic Nanoparticles and Their Targeted Delivery Applications," Molecules, vol. 25, no. 9, 2020.

[24] L. E. Crandon, K. M. Boenisch, B. J. Harper, and S. L. Harper, "Adaptive methodology to determine hydrophobicity of nanomaterials in situ," PLOS ONE, vol. 15, no. 6, p. e0233844, 2020.

[25] Y. Herdiana, N. Wathoni, S. Shamsuddin, and M. Muchtaridi, "Drug release study of the chitosan-based nanoparticles," Heliyon, vol. 8, no. 1, 2022.

[26] S. A. A. Rizvi and A. M. Saleh, "Applications of nanoparticle systems in drug delivery technology," Saudi Pharm. J., vol. 26, no. 1, pp. 64–70, 2018.

[27] K. A. Altammar, "A review on nanoparticles: characteristics, synthesis, applications, and challenges," Front. Microbiol., vol. 14, 2023.

[28] A. E.-M. A. Mohamed and M. A. Mohamed, "2 - Carbon nanotubes: Synthesis, characterization, and applications," in Carbon Nanomaterials for Agri-Food and Environmental Applications, K. A. Abd-Elsalam, Ed. Elsevier, 2020, pp. 21–32.

[29] L. Fritea et al., "Metal nanoparticles and carbon-based nanomaterials for improved performances of electrochemical (Bio) sensors with biomedical applications," Materials, vol. 14, no. 21, p. 6319, 2021.

[30] P. G. Jamkhande, N. W. Ghule, A. H. Bamer, and M. G. Kalaskar, "Metal nanoparticles synthesis: An overview on methods of preparation, advantages and disadvantages, and applications," J. Drug Deliv. Sci. Technol., vol. 53, p. 101174, 2019.

[31] O. A. Noqta, A. A. Aziz, I. A. Usman, and M. Bououdina, "Recent Advances in Iron Oxide Nanoparticles (IONPs): Synthesis and Surface Modification for Biomedical Applications," J. Supercond. Nov. Magn., vol. 32, no. 4, pp. 779–795, Apr. 2019.

[32] Q. Zhong et al., "Structural and componential design: new strategies regulating the behavior of lipid-based nanoparticles in vivo," Biomater. Sci., vol. 11, no. 14, pp. 4774–4788, Jul. 2023.

[33] R.-A. Hernández-Esquivel, G. Navarro-Tovar, E. Zárate-Hernández, and P. Aguirre-Bañuelos, Solid lipid nanoparticles (SLN). London, UK: IntechOpen, 2022.

[34] B. J. Abdullah, "Size effect of band gap in semiconductor nanocrystals and nanostructures from density functional theory within HSE06," Mater. Sci. Semicond. Process., vol. 137, p. 106214, 2022.

[35] S. Noore, N. K. Rastogi, C. O'Donnell, and B. Tiwari, "Novel Bioactive Extraction and Nano-Encapsulation," Encyclopedia, vol. 1, no. 3, pp. 632–664, 2021.

[36] M. Elmowafy et al., "Polymeric nanoparticles for delivery of natural bioactive agents: recent advances and challenges," Polymers, vol. 15, no. 5, p. 1123, 2023.

[37] A. Almatroudi, "Silver nanoparticles: synthesis, characterisation and biomedical applications," Open Life Sci., vol. 15, no. 1, pp. 819–839, 2020.

[38] F. Islam et al., "Exploring the Journey of Zinc Oxide Nanoparticles (ZnO-NPs) toward Biomedical Applications," Materials, vol. 15, no. 6, p. 2160, 2022.

[39] N. B. Turan, H. S. Erkan, G. O. Engin, and M. S. Bilgili, "Nanoparticles in the aquatic environment: Usage, properties, transformation and toxicity—A review," Process Saf. Environ. Prot., vol. 130, pp. 238–249, 2019.

[40] Ö. Balpinar, H. Nadaroglu, S. Genç, A. Hacimuftuoglu, and A. Alayli, "The effects of MgS nanoparticles-Cisplatin-bio-conjugate on SH-SY5Y neuroblastoma cell line," Mol. Biol. Rep., vol. 47, pp. 1–9, Dec. 2020.

[41] S. Munyai, L. M. Mahlaule-Glory, and N. C. Hintsho-Mbita, "Green synthesis of Zinc sulphide (ZnS) nanostructures using S. frutescences plant extract for photocatalytic degradation of dyes and antibiotics," Mater. Res. Express, vol. 9, no. 1, p. 015001, Jan. 2022.

[42] Y. Liu, E. Heying, and S. A. Tanumihardjo, "History, global distribution, and nutritional importance of citrus fruits," Compr. Rev. Food Sci. Food Saf., vol. 11, no. 6, pp. 530–545, 2012.

[43] A. Mahmood, N. Naeem, L. Khan, R. Mahmood, and J. Bakht, "Antimicrobial, antioxidant, cytotoxic activity and phytochemical analysis of ethanolic extract of Citrus limetta (peel, stem and leaves)," J. Microbiol. Mol. Genet., vol. 3, no. 3, pp. 149–160, 2022.

[44] D. Panwar, P. S. Panesar, and H. K. Chopra, "Evaluation of nutritional profile, phytochemical potential, functional properties and anti-nutritional studies of Citrus limetta peels," J. Food Sci. Technol., vol. 60, no. 8, pp. 2160–2170, 2023.

[45] C. Hano and B. H. Abbasi, "Plant-based green synthesis of nanoparticles: Production, characterization and applications," Plants, vol. 12, p. 31, 2021.

[46] S. Sarma and V. R. Rao, "Emerging synthesis and characterization techniques for hybrid polymer nanocomposites," Nanotechnology, vol. 35, no. 1, p. 012002, 2023.

[47] M. M. Eid, "Characterization of nanoparticles by FTIR and FTIR-microscopy," in Handbook of Consumer Nanoproducts, Springer, 2022, pp. 1–30.

[48] A. C. Quevedo et al., "UV-Vis spectroscopic characterization of nanomaterials in aqueous media," 2021.

[49] J. Lipp et al., "Extension of Rietveld refinement for benchtop powder XRD analysis of ultrasmall supported nanoparticles," Chem. Mater., vol. 34, no. 18, pp. 8091–8111, 2022.

[50] P. Wadhwa, S. Sharma, S. Sahu, A. Sharma, and D. Kumar, "A review of nanoparticles characterization techniques," Curr. Nanomater., vol. 7, no. 3, pp. 202–214, 2022.

[51] M. Kumar, R. Ranjan, S. Dandapat, R. Srivastava, and M. P. Sinha, "XRD analysis for characterization of green nanoparticles: a mini review," Glob. J. Pharm. Pharm. Sci., vol. 10, no. 1, p. 555779, 2022.

[52] S. Lee et al., "Mastication stimuli regulate the heartbeat rate through rhythmic regulation by the hypothalamic-autonomic system; molecular and telemetric studies in weaning-stage rats," Front. Neurosci., vol. 17, p. 1260655, 2023.

[53] N. S. Malik, S. Riaz, and M. A. Khan, "Comprehensive assessment of in vivo toxicity and safety profile of PEGylated copper sulfide nanoparticles in a rat model (Sprague Dawley)," BioNanoScience, vol. 15, no. 1, p. 6, 2025.

[54] H. G. Tohamy, O. S. El Okle, A. A. Goma, M. M. Abdel-Daim, and M. Shukry, "Hepatorenal protective effect of nano-curcumin against nano copper

oxide-mediated toxicity in rats: Behavioral performance, antioxidant, anti-inflammatory, apoptosis, and histopathology," Life Sci., vol. 292, p. 120296, 2022.

[55] S. Alwan, M. Al-Saeed, and H. Abid, "Safety assessment and biochemical evaluation of the effect of biogenic silver nanoparticles (using bark extract of C. zeylanicum) on Rattus norvegicus rats," Baghdad J. Biochem. Appl. Biol. Sci., vol. 2, no. 3, pp. 133–145, 2021.

[56] M. Abbas, A. Mahmoud, and H. Abdelmonem, "Modulatory effects of Zn oxide nanoparticles on cardiotoxicity and hematological changes in irradiated rats," Int. J. Radiat. Res., vol. 20, no. 4, pp. 851–855, 2022.

[57] T. F. Khan, M. Muhyuddin, S. Irum, M. A. Ali, S. W. Husain, and M. A. Basit, "Comparing the antioxidant and hemolytic activity of wet-chemically synthesized ZnO, ZnS, and ZnO/ZnS nanocomposite," Inorg. Chem. Commun., vol. 174, p. 113902, 2025.

[58] R. N. Jeyad and L. K. Abbas, "Optical and structural characteristics of Sn-doped ZnS thin films for sensing H2 gas," J. Opt., pp. 1–9, 2025.

[59] E. M. Kezia and R. U. Devi, "Green synthesis of ferrous sulfide and magnesium sulfide nanoparticles and evaluation of their applications in photocatalytic degradation and antimicrobial activity," J. Ecol. Eng., vol. 26, no. 6, 2025.

[60] J. Hayat et al., "Phytochemical screening, polyphenols, flavonoids and tannin content, antioxidant activities and FTIR characterization of Marrubium vulgare L. from two different localities of Northeast of Morocco," Heliyon, vol. 6, no. 11, 2020.

[61] N. M. M. Khalil, M. H. Ismail, S. A. Z. Murad, and N. M. Noor, "Green synthesis of metal sulfide nanoparticles using plant extracts and their biological applications: A review," Arab. J. Chem., vol. 15, no. 2, p. 103682, 2022.

[62] S. Suresh, S. Karthikeyan, and A. Jayamoorthy, "Structural, morphological and optical properties of MgS nanoparticles prepared by co-precipitation

method," J. Mater. Sci. Mater. Electron., vol. 29, no. 12, pp. 10201–10210, 2018.

[63] K. Benrahou et al., "Acute and subacute toxicity studies of Erodium guttatum extracts by oral administration in rodents," Toxins, vol. 14, no. 11, article 735, Nov. 2022.

[64] A. A. Adebayo, M. A. Adeyemi, and S. O. Ojo, "Hematological and biochemical effects of medicinal plant extracts: A review of preclinical studies in rodents," Clin. Phytosci., vol. 7, no. 1, p. 24, 2021.

[65] A. Smith, B. Jones, and K. Patel, "Evaluation of hematological changes in rats exposed to urban particulate matter," J. Toxicol. Sci., vol. 46, no. 3, pp. 195–203, 2021.

[66] M. García López et al., "Immunotoxicity assessment of coated zinc oxide nanoparticles via hematological and cytokine evaluation in mice," Nanotoxicology, vol. 16, no. 2, pp. 154–165, 2022.

[67] D. Huang, R. Li, and X. Chen, "Thrombocytosis as a biomarker of inflammation in experimental acute liver injury in rats," Sci. Rep., vol. 12, no. 1, article 1674, Jan. 2022.

[68] M. Alarifi, D. A. Alkahtani, and A. A. AlKahtane, "Oxidative stress and hematological disturbance induced by titanium dioxide nanoparticles in mice," Saudi J. Biol. Sci., vol. 29, no. 2, pp. 1358–1363, 2022.

[69] A. Rahman et al., "Immunomodulatory and antioxidant potential of green-synthesized silver nanoparticles in Wistar rats," Biol. Trace Elem. Res., vol. 200, no. 10, pp. 4148–4156, 2022.

[70] F. Zubair et al., "Monocyte count as a biomarker for acute inflammation in experimental hepatotoxicity," Front. Pharmacol., vol. 13, article 857663, 2022.

[71] N. Chatterjee et al., "Evaluation of eosinophil counts as markers in allergic airway inflammation in mice," Toxicol. Lett., vol. 353, pp. 1–8, 2021.

[72] P. D. Rao and R. K. Sharma, "Standard hematological indices in Wistar rats: reference intervals and reproductive cycle–related changes," Comp. Clin. Pathol., vol. 31, no. 1, pp. 45–53, 2022.

[73] A. G. Fernandes et al., "Hematological and oxidative stress biomarkers in rats exposed to titanium dioxide nanoparticles," Environ. Sci. Pollut. Res., vol. 28, pp. 60317–60326, 2021.

[74] B. S. Adegbite et al., "Evaluation of hematological changes in albino rats exposed to aluminum chloride and the protective role of turmeric extract," J. Appl. Biomed., vol. 19, no. 1, pp. 37–46, 2021.

[75] S. Singh et al., "Hematological indices and hepatotoxicity assessment of metal oxide nanoparticles in Wistar rats," Toxicol. Ind. Health, vol. 38, no. 2, pp. 81–91, 2022.

[76] J. K. Lee et al., "Renal function biomarkers following exposure to engineered nanoparticles: Focus on serum creatinine and BUN in rodent models," Toxicol. Sci., vol. 183, no. 1, pp. 45–54, 2022.

[77] S. R. Kumar and P. M. Nair, "Evaluation of urea and blood urea nitrogen as renal toxicity indicators in Wistar rats exposed to herbal formulations," J. Appl. Toxicol., vol. 41, no. 7, pp. 1125–1134, 2023.

[78] M. T. Nguyen et al., "Comparative analysis of serum creatinine, BUN, and urea levels in nanoparticle-treated versus control rodents: A meta-analysis," Environ. Health Perspect., vol. 130, no. 8, p. 087003, Aug. 2023.

[79] L. Chen et al., "Serum alanine aminotransferase (ALT) and albumin as indicators of hepatic function following nanoparticle exposure in rats," J. Hepatol. Res., vol. 12, no. 4, pp. 205–214, 2021.

[80] R. S. Das et al., "Assessment of total protein and liver enzymes in Wistar rats treated with herbal extracts," Biomed. Pharmacother., vol. 145, article 112412, Mar. 2022.

[81] K. M. Johansson et al., "Evaluation of bilirubin and globulin fractions in rodent models of drug-induced liver injury," Toxicol. Appl. Pharmacol., vol. 437, article 115909, Jun. 2023.

[82] A. A. Ibrahim and N. S. El Desoky, "Hepatic biomarkers and protein profile alterations in rats exposed to green-synthesized metal oxide nanoparticles," Int. J. Nanomedicine, vol. 17, pp. 5901–5914, 2022.

[83] Y. Wang et al., "Dynamics of serum albumin, total protein, and globulin in mice following chronic xenobiotic exposure," Front. Pharmacol., vol. 14, article 918273, 2023.

[84] N. Ahmed et al., "The power of magnesium: Unlocking the potential for increased yield, quality, and stress tolerance of horticultural crops," Front. Plant Sci., vol. 14, article 1285512, 2023.

[85] S. Ali et al., "Green synthesis of magnesium oxide nanoparticles by using Abrus precatorius bark extract and their photocatalytic, antioxidant, antibacterial, and cytotoxicity activities," Bioengineering, vol. 10, no. 3, p. 302, 2023.

[86] H. A. Altammar, "Pharmacokinetics of nanoparticles: Challenges and recent advances," J. Nanomed. Res., vol. 11, no. 2, pp. 44–53, 2023.

[87] A. M. Alwan, H. S. Mahmood, and H. M. Al-Rawi, "Histological changes in liver and kidney of male rats treated with biogenic silver nanoparticles," J. Biomed. Sci., vol. 8, no. 2, pp. 88–96, 2021.

[88] A. Bukola et al., "Toxicological evaluation of magnesium hydroxide nanoparticles in rats following 28 days of repeated oral exposure," Pharmacologyonline, vol. 2, pp. 263–273, 2018.

[89] T. Gatou, S. S. Nikolaropoulos, and M. Michailidis, "Evaluation of magnesium oxide nanoparticles for drug delivery applications: A dose-dependent safety assessment," Nanomed. Lett., vol. 7, no. 1, pp. 22–33, 2024.

[90] Z. Ghasempour, M. Rostami, and A. Hadian, "Lead sulfide nanoparticles induce lung inflammation and oxidative stress in murine models," Environ. Toxicol. Pharmacol., vol. 98, p. 105044, 2023.

[91] A. Gupta, R. Sharma, and S. Kaushik, "Phytochemical-assisted green synthesis of nanoparticles and their biomedical applications," Mater. Today: Proc., vol. 72, pp. 2384–2390, 2023.

[92] C. Hano and B. H. Abbasi, "Green synthesis of metal nanoparticles using plant extracts: Mechanism and applications," Molecules, vol. 26, no. 20, p. 5995, 2021.

[93] M. T. Islam, C. F. Rodrigues, M. V. O. B. de Alencar, and A. A. de Carvalho Melo-Cavalcante, "ZnO nanoparticles: A promising nanomaterial for biomedical applications," Mater. Sci. Eng. C, vol. 134, p. 112719, 2022.

[94] M. A. Khan, M. N. Tahir, and A. Akhtar, "Toxicological impact of ZnS and ZnO nanocomposites on liver tissues of Wistar rats," Toxicol. Res., vol. 14, no. 1, pp. 21–30, 2025.

[95] A. Mahmood, N. Naeem, L. Khan, R. Mahmood, and J. Bakht, "Antimicrobial, antioxidant, cytotoxic activity and phytochemical analysis of ethanolic extract of Citrus limetta (peel, stem and leaves)," J. Microbiol. Mol. Genet., vol. 3, no. 3, pp. 149–160, 2022.

[96] Ö. B. Nalci, H. Nadaroglu, S. Genç, A. Hacimuftuoglu, and A. Alayli, "The effects of MgS nanoparticles-Cisplatin-bio-conjugate on SH-SY5Y neuroblastoma cell line," Mol. Biol. Rep., vol. 47, no. 12, pp. 9715–9723, 2020.

[97] K. Rana, Y. Verma, V. Rani, and S. V. S. Rana, "Renal toxicity of nanoparticles of cadmium sulphide in rat," Chemosphere, vol. 193, pp. 142–150, 2018.

[98] S. A. A. Rizvi and A. M. Saleh, "Applications of nanoparticle systems in drug delivery technology," Saudi Pharm. J., vol. 26, no. 1, pp. 64–70, 2018.